DOKUZ EYLUL UNIVERSITY
GRADUATE SCHOOL OF NATURAL APPLIED SCIENCES

OBSERVATIONS OF THE PHYSICAL STRUCTURE AND NUTRIENT DISTRIBUTION OF THE CILICIAN BASIN, NORTHEASTERN MEDITERRANEAN SEA

by
İdil PAZI

September 2007
İZMİR

OBSERVATIONS OF THE PHYSICAL STRUCTURE AND NUTRIENT DISTRIBUTION OF THE CILICIAN BASIN, NORTHEASTERN MEDITERRANEAN SEA

A Thesis Submitted to
The Graduate School of Natural and Applied Sciences of Dokuz Eylül University
In Partial Fulfillment of the Requirements for the Degree of Doctor of Philosophy in
Institute of Marine Science and Technology, Coastal Engineering

by
İdil PAZI

September, 2007
İZMİR

Ph.D. THESIS EXAMINATION RESULT FORM

We have read the thesis entitled **"OBSERVATIONS OF THE PHYSICAL STRUCTURE AND NUTRIENT DISTRIBUTION OF THE CILICIAN BASIN, NORTHEASTERN MEDITERRANEAN SEA"** completed by **İDİL PAZI** under supervision of **Prof. Dr. FİLİZ KÜÇÜKSEZGİN** and we certify that in our opinion it is fully adequate, in scope and in quality, as a thesis for the degree of Doctor of Philosophy.

Prof. Dr. Filiz Küçüksezgin

Supervisor

Prof. Dr. Hüseyin Avni Benli	Prof. Dr. Baha Büyükışık
Committee Member	Committee Member
Yard. Doç. Dr. Mert Avcı	Prof. Dr. Temel Oğuz
Jury Member	Jury Member

Prof.Dr. Cahit HELVACI
Director
Graduate School of Natural and Applied Sciences

ACKNOWLEDGMENTS

I am grateful to Prof. Dr. Filiz KÜÇÜKSEZGİN for all her kind help and valuable comment during preparation of this study. I also wish to thank to Prof. Dr. Hüseyin Avni Benli for his creative discussion and also express our deep gratitude to Prof. Dr. Baha Büyükışık for helpful comments and constructive criticism of the manuscript. I also would like to thanks to Dr. Aynur KONTAŞ, Dr. Esin SUZER, Dr. Oya ALTAY, Enis DARILMAZ and Canan ERONAT for their valuable assistance to perform chemical and data analysis. I thank the crew of the *R/V K. Piri Reis* for their assistance during the fieldwork.

Great thanks are to my family for their encouragement and full support.

İdil PAZI

OBSERVATIONS OF THE PHYSICAL STRUCTURE AND NUTRIENT DISTRIBUTION OF THE CILICIAN BASIN, NORTHEASTERN MEDITERRANEAN SEA

ABSTRACT

The hydrographic characteristics were examined from three cruises in the Cilician Basin and reported, for the first time, on nutrient concentrations, ranges and distributions. The water mass, circulation and chemical properties of the Cilician Basin, the northeastern Levantine Sea, are described on the basis of three hydrographic cruises performed during May 1997 (spring), July 1998 (summer) and October 2003 (autumn). The hydrographic data reveal the presence of Levantine Surface Water (LSW) and Modified Atlantic Water (MAW) within the upper 90m layer, Levantine Intermediate Water (LIW) between 90 and 250 m, and Transitional Mediterranean Water (TMW) further below. During all sampling periods, there is no sign of a constant flow forming in the Cilician and Lattakia Basin. The variability of the circulation system is manifested by a change in shape, size and intensity of eddies as well as the direction of the Lattakia Basin coastal current system. It is only in October 2003, voluminous amounts of AW penetrated the region east of Cyprus at 40-50 m. The strong southward current at the east of Cyprus carried the AW to the Lattakia Basin. Statistical analysis of T-S relations indicate that; TMW frequency cover approximately 50% of all cases in all sampling periods. However, frequency of the other water masses changes due to seasonal thermohaline processes. The nutrient concentrations varied between nitrate+nitrite 0.16-0.31uM, phosphate 0.02-0.03 uM and silicate 0.95-1.2 uM for the surface layer during sampling periods. Dissolved nutrient concentrations in the Levantine Deep Water were: 2.1-5.3 uM for nitrat+nitrite, 0.10-0.21 uM for phosphate and 5.7-10 uM for Si. The molar ratios of nitrate to phosphate in the water column range between 5 and 20 in the surface layer and reach up to a value of 45 at the top of the nutricline at the depths of 29.05 sigma theta isopycnal surface for most of the year. Below the nutricline the N/P ratios retain the values around 24-28.

Keywords: water masses, circulation, dissolved nutrients, N/P ratio, Cilician Basin.

KUZEYDOĞU AKDENİZ KİLİKYAN BASENİ'NİN FİZİKSEL YAPISI VE NUTRİENT DAĞILIMININ İNCELENMESİ

ÖZ

Kilikyan Basenine ait hidrografik özellikler ilk kez nutrient konsantrasyonları oranları ve dağılımları ile birlikte incelenmiş ve rapor edilmiştir. Kuzeydoğu Levantin Denizi Kilikyan Basenine ait su kütlesi, sirkülasyon ve kimyasal özellikler Mayıs 1997 (ilkbahar), Temmuz 1998 (yaz) ve Ekim 2003 (sonbahar) tarihlerinde yapılan üç hidrografik deniz seferine dayanılarak tanımlanmıştır. Hidrografik veriler ışığında Kilikyan Baseninde 4 su kütlesi tespit edilmiştir: Yüzeyde Levantin Yüzey Suyu (LSW), 90 m'lik üst tabaka içinde değişikliğe uğramış Atlantik Suyu (MAW), 90-250 m arasında Levantin Ara tabaka Suyu (LIW) ve daha derinde değişime uğramış (transitional) Akdeniz Suyu (TMW). Tüm örnekleme periyodları boyunca Kilikyan ve Latakya Basenlerinde sabit bir akıntı tespit edilememiştir. Sirkülasyon sistemi, Latakya Baseni kıyı akıntı sisteminin yönü gibi, eddylerin şekil, boyut ve yoğunluğu açısından da değişiklik göstermektedir. Sadece Eylül 2003 seferinde Kıbrıs'ın doğusunda yaklaşık 40-50 m civarında yüksek hacimli AW girişi gözlenmiştir. Kıbrıs'ın doğusundaki güneye doğru oluşan kuvvetli akıntı AW Latakia Basenine taşımıştır. İstatistiksel T-S analizi sonucu, TMW örnekleme yapılan her mevsim için toplam su kütlesinin yarısını oluşturmaktadır. Bununla birlikte diğer su kütleleri thermohaline özelliklerinden dolayı mevsimsel değişimler göstermektedir. Örnekleme zamanına ait yüzey nutrient konsantrasyonları; nitrat+nitrit 0.16-0.31 uM, fosfat 0.02-0.03 uM ve silikat 0.95-1.2 uM değerleri arasında göstermektedir. Çözünmüş nutrient konsantrasyonları değişime uğramış Akdeniz Suyunda: nitrat+nitrit azotu için 2.1-5.3 uM, fosfat için 0.10-0.21 uM ve Si için 5.7-10 uM olarak ölçülmüştür. Su kolonunda yılın büyük bir kısmında nitratın fosfata molar oranı yüzeyde 5 ile 20 arasında, nutriklinin üstünde 29.05 yoğunluğa sahip tabakada 45 olarak hesaplanmıştır. Nutriklinin altında N/P oranı 24-28 arasında kalmıştır.

Anahtar sözcükler: su kütleleri, sirkülasyon, çözünmüş nutrientler, N/P oranı, Kilikyan Baseni

CONTENTS

Page

CHAPTER ONE
INTRODUCTION

1.1 Introduction

Scientific investigation is necessary in the adjacent seas of Turkey for both coastal manage development and conserve natural resources. Also it is most important that coastal economic development be generated for the people of a country, no just for those who are already rich and powerful. All countries around the Mediterranean Basin had made scientific investigations in their international water. On the other hand, scientific investigation that is as an example of development could not be realized in Turkish Republic of Northern Cyprus coastal waters because of its socio-economic condition.

The main purpose of this thesis is to explore the inter-seasonal variability of the local hydrography and to investigate the water masses, their seasonal and regional variations in the Cilician Basin based on data sets. In this thesis, the hydrographic data from cruise conducted in three different seasons in the Cilician Basin will be analyzed for the first time, on primary nutrient (nitrate, phosphate and silicate) concentrations, ranges and distributions. The joint analysis of temperature-salinity properties and chemical data also allows a better definition of water mass characteristics in the Cilician Basin and hints at basic mechanism relevant to water mass transformation and biological production in the Basin.

During the last decade and mainly within the framework of P.O.E.M. (Physical Oceanography of the Eastern Mediterranean) general features of the hydrology and circulation of the Levantine Basin and a more detailed water mass distribution have emerged (Ozsoy et al., 1993; Physical Oceanography of Eastern Mediterranean Group [POEM Group], 1992). However, little is known of the area north of Cyprus, which delineates our study area.

Although the nutrient regime of the eastern Mediterranean has been studied extensively in recent years the physical, chemical and biological data are too limited to reach reliable conclusions about the spatial and temporal variability of water masses in the Cilician Basin. It can be recognized that, these data from three cruises can provide an exhaustive description of water mass properties in the Cilician Basin. In addition to this, these data can serve a reliable basis for the future studies.

CHAPTER TWO
STUDY AREA

2.1 Description of the Study Area

The Mediterranean Sea, especially the eastern Basin, is a unique environment whose structure and function is poorly known. It is considered to be one of the most oligotrophic regions in the world with an overall nutrient deficit that develops towards the east (Ignatiades, 1969).

Cyprus is the third largest island in the Mediterranean Sea, located west of Syria and south of Turkey. The island has a maximum length of about 220 km from Cape Zafer in the northeast to the western extremity of the island. Its maximum width, from Cape Gáta in the south to Cape Kormakiti in the north, is about 90 km. The total area of the country is 9.251 km^2. Lefkoşa is the capital and largest city. Since 1974 the northern third of Cyprus has been occupied by Turkish troops and has formed a separate state called the Turkish Republic of Northern Cyprus.

The Cilician Basin lies in the northeastern part of the Mediterranean, between Northern Cyprus and the Turkish mainland. The smaller scale bathymetric features of the Levantine Basin are the Lattakia (1000-1500 m) and Cilician (1000 m). The relatively shallow Lattakia and Cilician Basins communicate with each other through a narrow channel of 700 m depth located nearly midway between the sills extending from the northeastern tip of Cyprus to the mouth of the Gulf of Iskenderun.

2.2 Geological Characteristic

The Levantine Sea is bordered on the north by Crete, the Dodecanese Islands and Turkey. On the east it is bordered by Syria, Lebanon and Israel and to the south by Egypt and Libya. The island of Cyprus is located in the northeast quadrant of the basin (Figure 2.1).

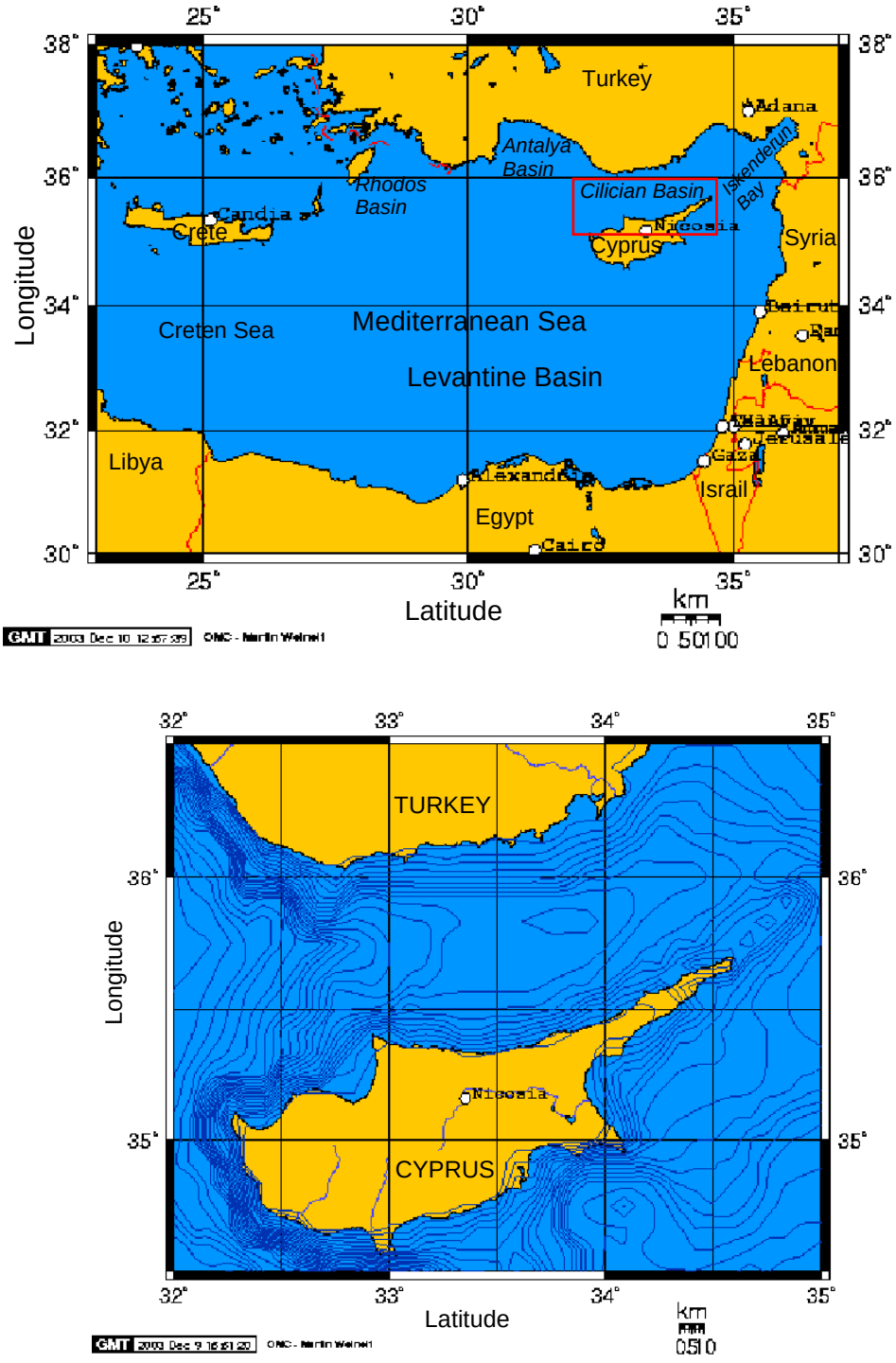

Figure 2.1 (a) Location of the Cilician Basin (b) The bottom topography of the Cilician Basin (The contour interval = 100 m) (http://www.aquarius.geomar.de/omc/make_map.html)

The margin of the basin includes an island arc from Crete through the Dodecanese Island to Rhodes. The remaining basin margins are of the less complex types consisting of continental shelves, slopes, rises and associated features. The predominant topographic feature of this region is the “Mediterranean Rise” (Carter et al., 1972).

Along the Turkish coast from the Rhodos channel eastward to Gelidonya Burun there is no significant continental shelf. From Gelidonya Burun to the northeastern corner of the Levantine Basin the average width is 4.5 km. A long this shelf the break varies from 40 m to 130 m in depth. Off the Gulf of Iskenderun a composite delta of several rivers has built a shelf 70 km wide. The shelf break is about 300 m deep along this portion of the shelf. The shelf is very narrow or absent at the Turkish-Syrian border. There is no significant island shelf along the southern coasts of the islands of the Cretan island arc. On the northern side of Cyprus the shelf averages 1 km wide and the shelf break is about 20 m deep. The southern coast has shelf width averaging 2 km and shelf break at 30 m (Carter et al., 1972).

Along the southern coast of Turkey the continental slope has a gradient ranging from 1:24 to 1:10. The slope is modified in the Gulf of Iskenderun by sediments from adjacent rivers. A north-west trending series of ridges and valleys, previously described as abyssal hills (Emery, Heezen and Allan, 1966), are seen along the eastern margin of the fan. These trends are parallel to a ridge, which connects the island of Cyprus and Anaximander Mountain south of the Turkish coast. A postulated transcurrent fault passing between Cyprus and Erathosthenes Tablemount (Wong, Zarudzki, Philips, and Giermann, 1971) also shows a similar trend. This series of ridges and valleys would seem to be structurally controlled.

The Cilician Basin is a small peripheral basin of the eastern Mediterranean (Biju-Duval, Letouzey and Montadert, 1979; Hsu & Bernoulli, 1978; Wong et al., 1971) located between the Cyprus and the southern Asia Minor (Turkish) coast. The basin is bounded to the north and south by the Taurus Mountains and Northern Cyprus coasts, respectively, and to the east by the Misis fault block, which forms a

submarine ridge between the Misis Mountains (Asia Minor) and the northeastern extremity of Cyprus (Evans, G., Morgan, Evans, W.E, Evans, T.R. and Woodside, 1978). The shelf bordering the Cilician Basin to the north is generally narrow, with the distance between the coast and the shelf break (located at ~200 m water depth; Ediger, Evans and Ergin 1997; Evans, Lane-Serff, Collins, Ediger and Pattiaratchi, 1995) being generally less than 15 km; however, offshore of the Seyhan/Tarsus/ Ceyhan deltaic system the shelf widens significantly, reaching a width of ~40 km. Two sub-marine canyons, the relief of which exceeds 200 m at some sections, are present offshore Erdemli. These canyons, which may represent major conduits for sediment transfer from the Mersin Shelf to the deep environments of the Cilician Basin, merge on the lower slope at 850 m water depth to produce a single canyon (Figure 2.1). The continental shelf bordering the Cilician Basin to the north has a low relief except for some minor irregularities (a few meters in scale) on the mid-shelf, which are considered to be old coastal barriers cloaked by modern sediments (Evans et al., 1995). Shelf sediments consist of terrigenous sediments inshore and shells/shell debris at the mid-shelf (at water depths of 50-100 m), whereas pro-deltaic sediments are found offshore of the Seyhan/Tarsus/Ceyhan and the Goksu rivers (Figure 2.1). The outer shelf, between the 100 m bathymetric contour and the shelf edge, is associated with fine sediments with abundant planktonic skeletal debris, whereas the surficial sediments of the continental slope and basin consist of clayey silts and silty clays (Aksu et al., 1992; Ediger et al., 1997; Shaw, 1978; Shaw and Bush, 1978). Seven depositional units, considered to represent different progradational phases of the deltaic systems of the area during the Quaternary, have been identified above the acoustic basement at the Cilician continental margin; their total age is interpreted to be 0.6 Myr (Aksu et al., 1992).

2.3 Previous Studies

The Mediterranean Sea is well known to be one of the most oligotrophic regions in the world with an overall nutrient deficit that develops towards to east (Bethoux & Copin-Montegut, 1988; Bethoux, Morin, Madec and Gentili, 1992; Coste, Le Corre, and Minas 1988; Krom et al., 2004; Loye-Pilot, Martin and Morelli, 1990; McGill, 1969; Redfield, Ketchum and Richards, 1963). In the Mediterranean Sea, unlike in

other ocean basins, phosphates, as opposed to nitrates, those are considered to be the factor limiting phytoplankton growth (Becacos-Contos, 1977; Krom, Kress and Brenner 1991; Krom et al., 1992; MacIsaac & Dugdale, 1972; Thingstad & Rassoulzadegan, 1995).

While the general features of the hydrology and circulation of the Eastern Mediterranean are fairly well recognized (Ozsoy, Hecht and Unluata, 1989; Ozsoy et al., 1991; POEM Group, 1992), a consistent representation of their characteristics in the Cilician Basin, which delineates our study area (Figure 2.1), is still lacking. The analysis of the water masses and circulation system may provide a better understanding of the basic futures and processes of the Cilician Basin.

Analysis of data collected during the multinational POEM programme (Brenner, Rozentraub, Bishop and Krom, 1991; POEM Group, 1992; Robinson et al., 1987) has shown that the circulation in the Levantine Basin is composed of a complex series of sub-basin-scale gyres, jets and energetic mesoscale eddies. Similar conclusions were drawn by Hetch, Pinardi and Robinson (1988) based on data from the 17 Marine Climate cruises (MC) during the period 1979-1984. Based on Physical Oceanography of the Eastern Mediterranean (POEM) data in the region Ozsoy et al. (1991, 1993), POEM Group (1992), Robinson et al. (1991) identified the major water circulation feature of the study area. Mid Mediterranean Jet (MMJ), approaching Cyprus from the south bifurcates to the island’s southwest. One of the branches flows northward becoming the Asia Minor Current (AMC) and finds its way to the Antalya Basin.

The other branch separates, flows east and turns southward. Sometimes a bifurcation occurs with flow around Cyprus into the Cilician Current (CC). The Cilician basin is as representative of an anticyclonic region where in general small scale eddies are observed (Yilmaz and Tugrul, 1998). General circulation of the Mediterranean Basin agrees with observational evidence of seasonal cycle of the basin and perhaps the interannual components of the flow (Roussenov, Stanev, Artale, and Pinardi, 1995).

Deep anticyclonic eddies in the eastern Mediterranean Basin consist of warm salty (>39.05%) water. Life-time of eddies could be several years, and up to three or four could form annually. It is suggested that the eddies probably form along the coasts of Asia Minor and move first southwards and then eastwards (Felix and Itzikowitz, 1987).

The characteristics water masses of the Levantine Basin are the Levantine Surface Water (LSW) within the mixed layer during highly stratified seasons, the Modified Atlantic Water (MAW) reaching the Levantine Basin from the Atlantic Ocean, the Levantine Intermediate Water (LIW), which is locally produced in the northern Levantine basin and the Levantine deep water (LDW) (Ozsoy et al., 1989). In the deep layers, the Transitional Mediterranean Water (TMW) can be detected by its low salinity (~38.9) (~300-600m), located between the LIW and Eastern Mediterranean Deep Water throughout the entire Eastern Mediterranean (Theocharis, Balopoulos, Kioroglou, Kontoyiannis and Iona, 1999; Tselepides, Zervakis, Polychronaki, Danovaro and Chronis, 2000). The LIW is exclusively produced in several areas in the Levantine Basin and the Southern Aegean Sea, during February and March, under the influence of dry and cold continental air masses (Ovchinnikov, 1984; Unluata, 1986) and can be found in pools trapped within anticyclonic eddies and along the Anatolian coasts (Brenner et al., 1991; Ozsoy et al., 1989, 1991, 1993). The intense research during the last 15 years in the Eastern Mediterranean Basin revealed significant details of the thermohaline circulation and its abrupt change that occurred in the last decade (Lascaratos, Roether, Nittis and Klein, 1999; Malanotte-Rizzoli et al., 1999; Ozsoy et al., 1993; Roether et al., 1996; Theocharis, Georgopoulos, Lascaratos and Nittis, 1993; Theocharis, Klein, Nittis and Roether, 2002).

LIW is exclusively produced in several areas in the Levantine Basin and the Southern Aegean Sea, during February and March, under the influence of dry and cold continental air masses (Ovchinnikov, 1984; Unluata, 1986) and can be found in pools trapped within anticyclonic eddies and along the Anatolian coasts (Brenner et al., 1991; Ozsoy et al., 1989, 1991, 1993). Both the intermediate and deep conveyor belts of the Eastern Basin presented rather constant characteristics (Lascaratos et al.,

1999; Malanotte et al., 1999; Ozsoy et al. 1993; Roether et al., 1996; Theocharis et al., 2002) indicating an almost perfectly repeating cycle in both water mass characteristics and formation rates during the last 20 years.

Before 1970 nitrate data were scarce in the Mediterranean Sea, particularly in the western Basin, and it, therefore, is not possible to prove an evolution of nitrate concentration in the deep water as phosphate (Bethoux et al., 1992). The N/P molar ratio was found to vary between 20 and 23 in both the eastern and western basins (Bethoux & Copin-Montegut, 1988; Bethoux et al., 1992; Salihoglu et al., 1990) in contrast to a molar ratio of 16 in the ocean, from Redfield at al. (1963). Phosphate limitation of the eastern Mediterranean was further supported by Krom et al. (1992, 1993) by the observations in the warm-core Cyprus eddy, located to the south of Cyprus. According to Yilmaz and Tugrul (1998), the nutrient distribution and phytoplankton production in the Levantine Sea of the Eastern Mediterranean are principally determined by the duration and the intensity of deep winter mixing in the quasi permanent anticyclonic and cyclonic eddies. The Levantine deep waters have relatively high N/P ratios (~28), greatly exceeding the oxidative ratios of nitrate to phosphate in the deep oceans (Takahashi, Broecker and Langer, 1985). Yilmaz and Tugrul (1998); determined relatively low N/P ratios –with respect to Redfield ratios- in biogenic particles from the Levantine surface layer, they suggest that there should be another source for the observed high N/P ratios in the LDW. The most probable source is the sinking water, selectively enriched with labile dissolved organic, inorganic nitrogen constituents (Yilmaz and Tugrul 1998).

2.4 Impact of Desert Dust on the Cilician Basin

Pulses of mineral aerosols originating from North Africa reach the Mediterranean region, and their micro- (such as Fe, Zn, Mn, Co, Ni) (Kubilay, 1996) and macro-nutrient (such as PO_4^{-3} and NO_3^-) content (Bergametti et al., 1992; Migon & Sandroni, 1999; Talbot et al., 1986) supposedly could contribute to marine biological production through time-dependent biogeochemical processes (Quetel et al., 1993). Among these nutrients, PO_4^{-3} is known to be the limiting nutrient for phytoplankton production in the Mediterranean and as a result of this limitation Eastern

Mediterranean marine environment is characterized with a high N:P ratio near the sea surface (Krom et al., 1991).

Kubilay, Nickovic, Moulin and Dulac (2000) focus on the long-range transport of African dust to the eastern Mediterranean, to describe the meteorological processes creating it, and the seasonal variability of its deposition on the Turkish coast. Ground-based measurements, satellite data and modeling could be used to estimate the mass of desert dust in the eastern Mediterranean atmosphere (Kubilay et al., 2000).

In order to define deposition atmospheric fluxes of macro-nutrients into the Cilician Basin waters absorbing aerosol index was used from NASA web site ftp://jwocky.gsfc.nasa.gov/pub/tmp/meduse/. Aerosol index data were provided by the Earth Probe/Total Ozone Mapping Spectrometer (EP/TOMS) and utilized to designate the specific dust sources around the eastern Mediterranean during the cruises and 20 days ago. Aerosol dust distributions inferred by TOMS aerosol index data during the cruises (and 20 days ago) suggest that the whole Clician Basin is not loaded with desert dust.

2.5 Impact of Global Warming

The LIW is exclusively produced in several areas in the Levantine Basin and the Southern Aegean Sea, during February and March, under the influence of dry and cold continental air masses (Ovchinnikov, 1984; Unluata, 1986).

While the LIW occurred at the depth of 300 m in 1991 (Ozsoy et al., 1992; 1993), it extending up to ~200 m after 1995, with a temperature of about 16°C and constant salinity (S=39.2 psu) in our sampling periods. Zodiatis et al. (1998) also found the similar results in summer 1995 and spring 1996 surveys. The depth of LIW is indicated an inter-annual trend because of global warming. Figure 2.2 (a) and (b) show that yearly average air temperature and monthly average air temperature in February and March from 1980 to 2006 from the Mediterranean coast.

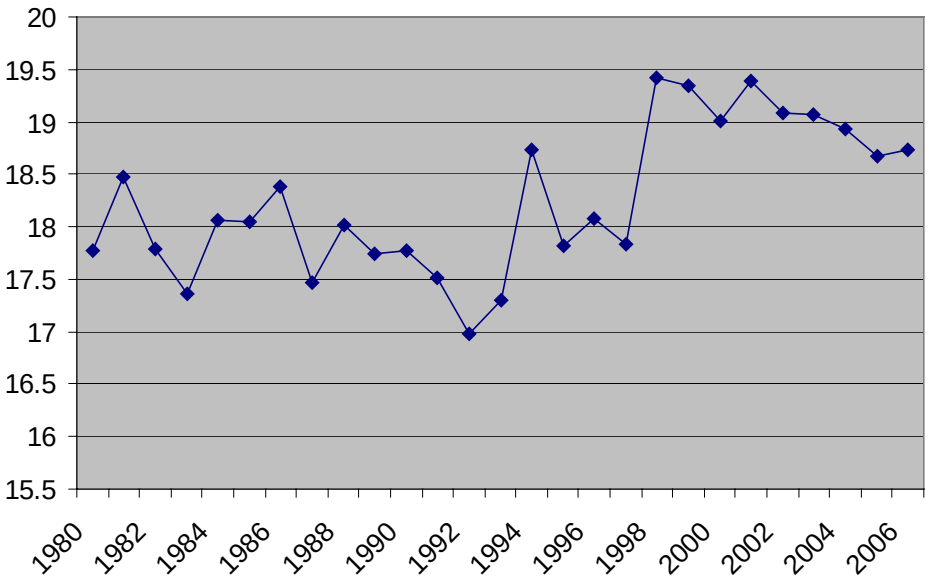

a

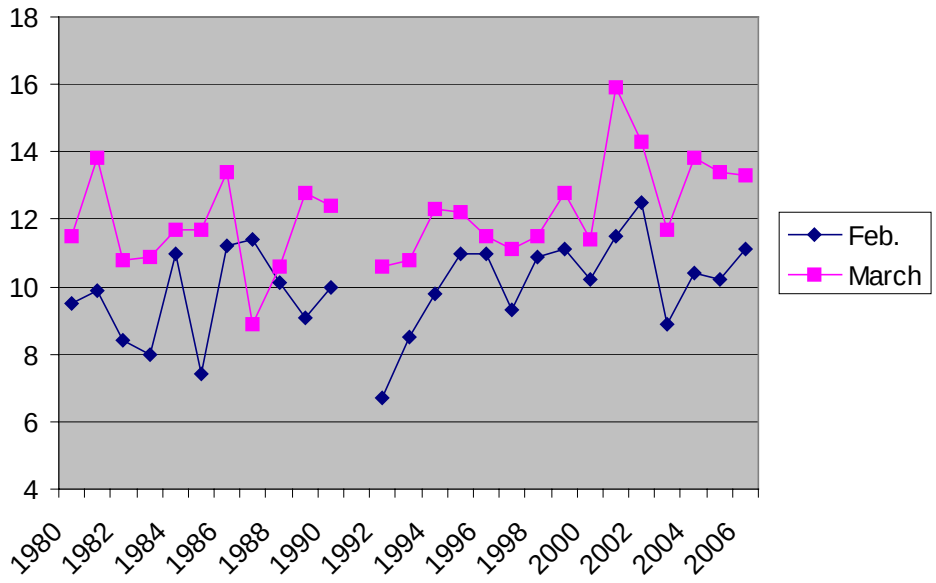

b

Figure 2.2 (a). Yearly average air temperature (°C) and (b) Monthly average air temperature (°C) in Antalya (from Antalya Meteorological Station)

CHAPTER THREE
MATERIALS AND METHODS

3.1 Materials

The investigation was restricted to an area 180 by 80 km on the northern Levantine part of the Eastern Mediterranean. The data were collected as part of three cruises of the R/V *K. Piri Reis* in May 1997, July 1998 and October 2003 within the framework of a 'Bio-ecological Properties of the Surrounding Waters of the Turkish Republic of Northern Cyprus' Project (Figure 3.1) (IMST, 1998; 1998; 2003). Data summary were given in Table 3.1.

Table 3.1 Data summary

Cruise	Date	Number of CTD Stations
May 1997	10-20 May 1997	29
July 1998	12-17 July 1998	38
October 2003	19 Oct.-3 Nov. 2003	39

During each cruise, standard CTD profiles were obtained at each station using a SBE-9 CTD, equipped with pressure, temperature, conductivity, dissolved oxygen and light transmission sensors, and water samples were collected from discrete depths using a General Oceanics Rosette sampler attached to the CTD. The CTD salinities were calculated using the 1978 Practical Salinity Scale equations (1980). Sea Bird CTD sensors were calibrated by the northwest Regional Calibration Center (operating under contract to NOAA) once a year. The characteristics of sensors the employed are given on Table 3.2.

Water for nutrient samples was collected as soon as the rosette was taken on board. Samples were collected in 100 ml polyethylene bottles, which had been pre-washed with 10% hydrochloric acid. At the time of sampling the sample bottles were

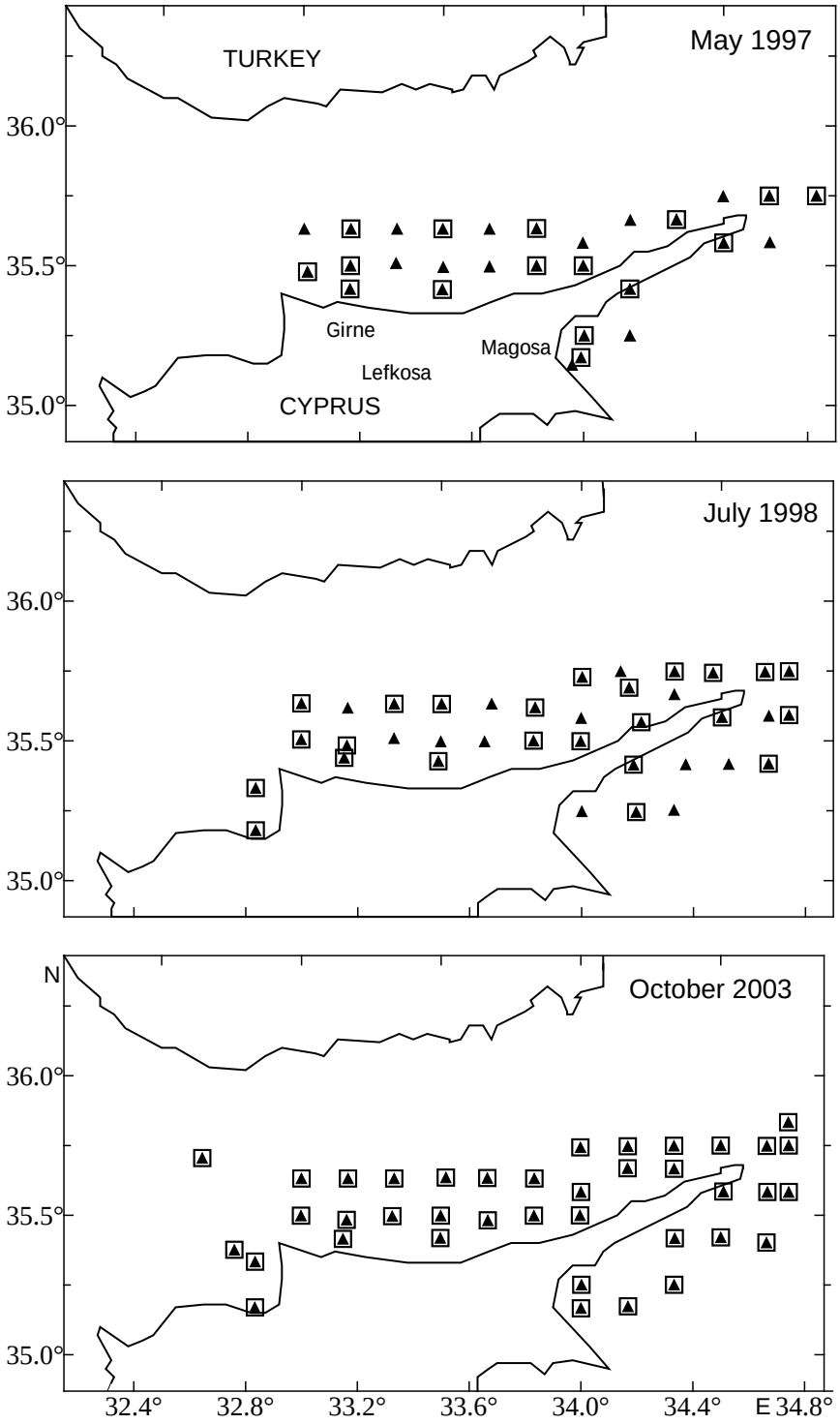

Figure 3.1 Location of stations in the Cilician Basin. The stations are plotted with different symbols where ▲ and □ show hydrographic and nutrient stations respectively

Samples were kept continuously in deepfreeze (-20°C) until analysis. Sample determinations were generally carried out within one week of the completion of the cruise (Stricland and Parsons, 1972; Grasshoff, Ehrhardt and Kremling, 1983).

Table 3.1 Properties of SBE 911plus CTD system sensors

Parameter	Measurement range	Accuracy	Resolution
Pressure	0 to 3000 psi	0.015% of full scale	0.001% of full scale
Temperature	-5 to +35°C	±0.001°C	0.0002°C
Conductivity	0 to 7 S/m	±0.0003 S/m	0.00004 S/m
Dissolved Oxygen	0 to 15 ml/l	±0.1 ml/l	±0.01
Light Transmission	0-100	±0.025	

3.2 Methods

The main hydrographic structures of the Cilician Basin and zonation of local water masses will be discussed in this study in terms of temperature, salinity and nutrients. The water mass properties during the considered period will be summarized in a θ-S (potential temperature-salinity) diagram where we can distinguish the characteristics of water column. The maps of geostrophic current vectors have been constructed by the employment of dynamic method using 450-500 m reference levels, which is calculated by Defant's idea (Defant, 1941). The relative current at 400-500 m depths is most likely to equal zero. Mean nutrient concentrations in this context should correspond to the depth intervals defined according to the values and ranges for T, S and density. Composite profiles obtained from the basin-wide chemical data will be plotted against temperature, salinity and water density permit us to define the boundaries of hydro-chemically different water masses in the Clician Basin.

3.2.1 Vertical Profiles

A vertical profile is a graph showing how some property (temperature, salinity, etc.) varies with depth in the ocean. Two of most important properties of seawater are temperature and salinity, for together they control its density, which

is the major factor governing the vertical movements of ocean. Salinity varies throughout the oceans depends almost entirely on the balance between evaporation and precipitation and the extent of mixing between surface and deeper waters. Zones where salinity decreases with depth are typically found at low and middle latitudes, between the mixed surface layer and the top of the deep layer, in which the salinity is roughly constant. These zones are known as haloclines; the term applies also to zones where salinity increases with depth (whereas in thermocline temperature almost invariably decreases with depth). Generally, haloclines and thermoclines are identified by pynoclines, which the density changes sharply.

Above the permanent thermocline, the distribution of temperature with depth shows seasonal variations, especially in mid-latitudes. During the winter, when surface temperatures are low and conditions at the surface are rough, mixed surface layer may extend to the permanent thermocline; i.e. the temperature profile can be effectively vertical through the top 200-300m or more. In summer, as surface temperatures rise and conditions at the surface are less rough, a seasonal thermocline often develops above the permanent thermocline. Seasonal thermoclines start to form in spring and reach their maximum development in the summer. They develop at depths of a few ten of meters, with a thin mixed layer above. Winter cooling and strong winds progressively increase the depth of seasonal thermoclines and reduce the temperature gradient along them; eventually the mixed layer reaches its full thickness of 200-300m. In low latitudes, there is no winter cooling, so the ‘seasonal thermocline’ becomes ‘permanent’ and merges with the permanent thermocline at depths of 100-150m. At high latitudes greater than about 60° there is no permanent thermocline (The Oceanography Course Team, [OCT] 1997 p.34)

3.2.2 *T-S Analyses*

The analysis of T-S relationships, together with the field expressing the equation of state of sea water, allows us to take into account the most important factors

which determine the nature of the transformation and interaction of different water mass; in particular, the family of isopycnals allows us to take account of the effect of contraction on mixing of sea waters. Before turning directly methods of thermohaline analysis, we should draw up a classification of the types of T-S relations, which can be plotted, on the diagram (Mamayev, 1975, p. 247).

3.2.2.1 Water Masses and Thermohaline Index

The concept of primary water masses homogeneous in temperature and salinity (which can be represented on the T-S diagram in the form of individual thermohaline indexes), which underlies the analytical theories of T-S curves and the methods of their analysis, does not correspond, as has already been said, to reality for in the World Ocean we observe continuous distribution of temperature and salinity vertically and horizontally. On the other hand, a kind of generalization of the concept of the water mass is possible within the framework of T-S analysis; by water mass we do not necessarily have to refer to a discrete volume of water existing in the ocean, homogenous or almost homogenous in temperature and salinity. If say, stationary values of temperature and salinity are observed on the surface of the ocean in some point, the corresponding thermohaline index may be considered an indicator of the water mass. Isolating the termohaline indexes of the original “pure” water masses is necessary not only in order to define the boundaries between the water masses, but also to determine the percentage content of the waters and other numerical characteristics of interaction of water masses (Mamayev, 1975, p.250).

3.2.2.2 Analysis of Water Masses using the T-S Curves

The most common case of mixing of water masses under the real conditions of the World Ocean is the vertical mixing of two, three or four superimposed water masses. The basis for the study of the vertical mixing of waters on the T-S diagram is the analytical theory of T-S curves for an ocean. The practical outcome of the analytical theory of T-S curves took the form of seven

fundamental theorems of the “geometry of T-S curves”. These rules were proposed by Sthokman (1944) and they may be stated in the following way:

1. The boundary between two water masses should be considered the depth at which the percentage content, as determined by the straight line of mixing or the triangle of mixing amounts to 50% for each of the water masses.
2. If the T-S curve is close to straight line, then the straight line of mixing should be used for its analysis. In this case, the indexes of the two mixing water masses lie on the ends of the curve and correspond to the surface and deep-water masses.
3. If the T-S curves consist of two or more straight (or almost straight) sections, connected among each other, then there are three or more water masses. The quantity of water masses is equal to the quantity of water extremes (or conjugations) plus two.
4. The determination of the T-S indexes is made by drawing tangents to the straightened out sections of the T-S curve. In this case the intersection of the tangents in the region of the extreme (conjugation) indicates the T-S index of the intermediate water mass; the ends of the branches of the T-S curve correspond to the surface and bottom water masses.
5. For the determination of the boundaries and percentage content of the water masses at different depths, triangles of mixing are plotted on the T-S indexes as apexes.
6. The principal median of the triangle of mixing drawn from that apex which corresponds to the intermediate water mass to the middle of the opposite side (called the base of the triangle of mixing), intersects the T-S curve in that point where parameter z characterizes the position of the core of the intermediate water mass.
7. The secondary medians of triangle of mixing, drawn from the middle of the base of the triangle of mixing to the other two sides, intersects the T-S curve in those points of it where parameter z corresponds to the boundaries of the intermediate water mass. The part of the T-S curve contained between the

secondary medians of the triangle of mixing corresponds to the intermediate water mass (Mamayev, 1975, p.252).

3.2.2.3 Statistical T-S Analysis

….The subject of statistical T-S analysis is the frequency of observations, which correspond to definite points on the T-S diagram or definite squares on it. The study of the frequency of T-S relations, broken down in a certain way into classes by temperature and salinity, may be carried out by time, by space and finally by volume. Statistical T-S analysis has considerably expanded the possibilities of T-S analysis as whole; the later was applied earlier, as we have seen, primarily to individual T-S curves (Mamayev, 1975, p.295).… All observations of temperature and salinity were broken down into intervals of 1°C for temperature and 0.1‰ for salinity in this study. In the corresponding squares of the T-S diagram was inscribed the frequency of the observations. Thus, frequency indicates the corresponding part of the total area in which temperature and salinity are observed simultaneously at given intervals.

3.2.3 Baroclinic Rossby Radius of Deformation

The horizontal scale, which establishes dimensions of the boundary of any oceanic flow that is strongly influenced by rotation is the Rossby radius of deformation, or more simply, the Rossby radius. There are actually two types of Rossby radiii, one for barotropic flow and one for the baroclinic flow…..Consider a cross-stream section in a two-layer configuration shown shematically in Figure 3.1. The upper layer is assumed to be of variable height, $\xi(x)$, while the lower layer is quisescescent and very deep. ρ_1 is the surface layer density and ρ_2 is located between the surface the secon underlying layer of constant density (Apel, 1987, p.311).

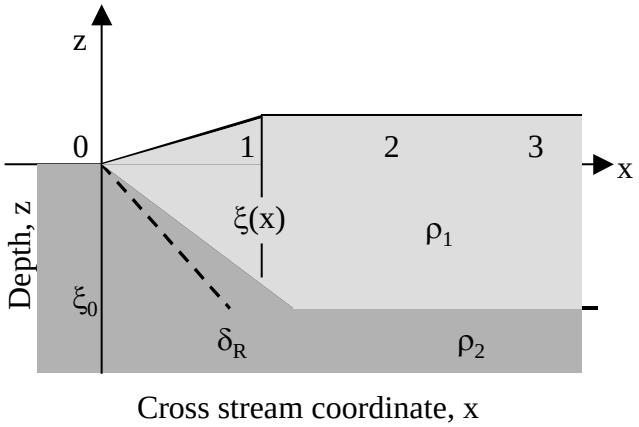

Figure 3.1 Schematic cross section of baroclinic flow and the Rossby radius δ_r establishes on the x scale (Apel, 1987, p.311).

$$\delta_R = (1/f)(g'*\xi_0)^{1/2}$$

$$g' = \frac{\rho_2 - \rho_1}{1/2(\rho_2 + \rho_1)}$$

$$f = 2\Omega \sin 35.5 \text{ for Cilician Basin}$$

Thus it can be seen that δ_r is the ratio of the speed of a shallow water internal gravity mode, $(g'\xi_0)^{1/2}$, in a layer of thickness, ξ_0, and reduced gravity, g', to the Coriolis frequency (Apel, 1987, p.313). The horizontal dimensions of a phenomenon were characterized by internal radius of deformation ≈ 10-14 km in the Cilician Basin.

3.2.4 Geostrophic Currents

When a frictionless current flows horizontally without change of velocity and the only external force is gravity, for each horizontal coordinate direction the components of the coriolis force and the pressure gradient force balance each other. In the vertical direction the pressure gradient is balanced by the vertical component of the coriolis force and the gravitational force.

$$2\omega \sin\phi \cdot \rho v = \frac{\partial p}{\partial x}$$

$$2\omega \sin\phi \cdot \rho u = -\frac{\partial p}{\partial y} \qquad (1)$$

$$2\omega \cos\phi \cdot \rho u = -\frac{\partial p}{\partial z} + g\rho$$

The term $2\omega\sin\phi.\rho u$ in most ocean currents can be neglected in the third of eq.1, and hydrostatic equilibrium is approximated by the hydrostatic equation $\partial p = g\rho \partial z$. The equation of continuity is satisfied for a stationary mass distribution ($\partial\rho/\partial t = 0$).

If the first and second of eq.1 are squared and added together, the result can be written:

$$\frac{\partial p}{\partial n} = 2\omega \sin\phi \cdot \rho c \qquad (2)$$

where:

$$c = (u^2 + v^2)^{1/2} \text{ and } \frac{\partial p}{\partial n} = \left[(\partial p/\partial x)^2 + (\partial p/\partial y)^2\right]^{1/2}$$

that equilibrium of forces as shown in eq.2 expresses the fact that the coriolis force must be equal and exactly opposite to the horizontal pressure gradient force. This means that the horizontal current vector, c, must be parallel to the isobars, and in such a direction that in the Northern Hemisphere, the higher pressure is to the right when one faces in the direction of the current. In the Southern Hemisphere, where ϕ is counted as a negative quantity, the higher pressure is to the left when looking “downstream”. This type of current is called geostrophic current and equilibrium of forces expressed by eq.2 is called a geostrophic equilibrium.

Instead of using horizontal pressure gradient along level surfaces, the slope of isobaric surfaces can be introduced in eq.2. Figure 3.3 represents two isobars in a vertical plane, p and $p + \Delta p = p + \rho g \Delta z$ where ρ is the density of water column between points B and C. thus

$\Delta p / \Delta n = \rho g (\Delta z / \Delta n)$ and:

$$\frac{\partial p}{\partial n} = \rho g \tan\beta \qquad (3)$$

A negative sign on the right side of eq.3 has to be used when the z-axis points downward in a positive direction. In this case, β is positive in the clockwise direction. If eq.3 is introduced into eq.2, it follows that:

$$\tan\beta = \frac{2\omega\sin\phi}{g}c \qquad (4)$$

In the Southern Hemisphere, the slope reverses since the coriolis term changes sign and the isobaric surfaces slope upward to the left when one faces in the direction of current c (Neumann, 1968, p. 127).

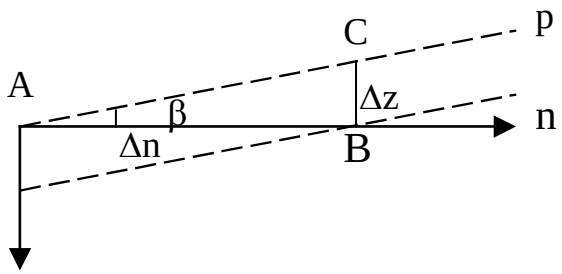

Figure 3.3 Two isobars, p and p+Δp, in the vertical nz-plane (Neumann, 1968, p. 129)

3.2.4.1 Practical Application of the Geostrophic Equilibrium

Consider two oceanographic stations, A and B, for which the distribution of density with depth is known from observations of T and S with depth. The dynamic height difference D, in dynamic meters between two isobaric surfaces p_1 and p_2 between adjacent stations depend only on the terms that contain the anomaly of the specific volume. Variations in dynamic height are described as **dynamic topography**. Thus:

$$D_A - D_B = \Delta D_A - \Delta D_B = \int_{p_1}^{p_2} \delta_A dp - \int_{p_1}^{p_2} \delta_B dp \qquad (5)$$

the horizontal pressure gradient in eq.2 can be expresses in terms of the slope of isobaric surfaces according to eq.3. Introduction of dynamic depth in units of the dynamic depth in units of a dynamic meter yields:

$$\frac{\partial p}{\partial n} = -\rho g \frac{\partial D}{\partial n}$$

and

$$2\omega \sin\phi c = -g\frac{\partial D}{\partial n} = -g\frac{\Delta D_A - \Delta D_B}{\Delta n} \qquad (6)$$

where Δn is the horizontal distance when proceeding from station A to station B in the positive n-direction. Since ΔD_A and ΔD_B represent the (relative) dynamic depth anomaly between isobaric surfaces, the velocity $c=c_1-c_2$ can also represent only the relative velocity between two isobaric surfaces p_1 and p_2. Thus for practical uses, eq.6 can be written:

$$c_1 - c_2 = \frac{g}{2\omega \sin\phi \cdot \Delta n}(\Delta D_A - \Delta D_B) \qquad (7)$$

the velocity difference, c_1-c_2, is obtained in cm/s if the dynamic depth difference is expressed in dynamic cm, and Δn in cm.

In order to arrive at absolute currents, either the absolute pressure field or the absolute current velocity must be known with sufficient accuracy at least at one level in the sea such a level is called reference level. Since the inclination of isobaric surfaces against level surfaces is very small, no method exists in oceanography at present to measure this inclination directly. Direct current measurements at sea are quite difficult. In the past oceanographers have tried to find a zero level or level of no motion in the ocean by indirect evidence. Several suggestions have been offered and attempts have been made to find evidence for a motionless or nearly motionless layer beneath the sea surface. Among the existing methods, it appears that Defant's (1941) approach is most practical. Essentially, Defant starts with the hypothesis that it is more reasonable to assume that the strongest currents occur in the upper, most strongly stratified strata of the sea. Upon comparing the differences of the relative dynamic depth of given isobaric surfaces between adjacent oceanographic stations, it is found that in some deep-sea layers this difference was practically constant over a rather large depth interval. It seems unreasonable to assume that these deep layers are moving with uniform speed and that the surface layers are almost motionless. Thus, Defant suggested that these deep layers with constant or nearly constant

horizontal pressure gradients are motionless in horizontal direction, rather than at uniformly high speed as compared to the surface (Neumann, 1968, p. 135).

3.2.5 Nutrient

(Nitrate+Nitrite)-nitrogen (NO_3+NO_2)-N, o-phosphate phosphorus (o.PO_4-P), silicate [$Si(OH)_4$] were measured spectrophotometrically using cadmium reduction method, ascorbic acid method, molybdosilicate method, respectively (Grasshoff, Ehrhardt and Kremling, 1983; Strickland and Parsons, 1972). Intercalibration seawater samples (from QUASIMEME, Plymouth Marine Laboratory, Round 22 and 28) were used as a control for the analytical methods. The values obtained (in μM) for the analyses of ten replicates of this sample were as follows: (NO_3+NO_2)-N (certified 8.68±0.38; found 8.78±0.04), o.PO_4-P (certified 0.76±0.05; found: 0.78±0.008), Total PO_4-P (certified 0.88±0.08; found: 1.0±0.07), [$Si(OH)_4$] (certified 3.93±0.48; found: 4.18±0.05).

Nitrate+Nitrite Nitrogen: Nitrate+Nitrite is based on the hydrazinium reduction method; nitrate is reduced to nitrite by hydrazinium sulfate and the nitrite is determined by diazotizing with sulfanilamide and N-(1-naphtyl)-ethylenediamine to form a highly colored azo dye in automated system (Stricland and Parsons, 1972) (Detection limit: 0.1 μM).

Nitrite Nitrogen: (NO_2-N) in the seawater is allowed to react with sulphanilamide in an acid solution. The resulting diazo compound reacts with N-(1-naphtyl)-ethylenediamine and forms a highly colored azo dye (Stricland and Parsons, 1972) (Detection limit: 0.01 μM).

Orto Phosphate Phosphorus: The seawater sample is allowed to react with a composite reagent containing molybdic acid, ascorbic acid and trivalent antimony. The resulting complex heteropoly acid is reduced in situ to give a blue solution, the extinction of which is measured at 880 nm (Grasshoff, Ehrhardt and Kremling, 1983).

Reactive Silicate: The seawater sample is allowed to react with molybdate under acidic conditions, which result in the formation of the silicomolibdic acid. A reducing solution, containing ascorbic acid, is then added which reduces the silicomolybdate complex to give a blue reduction compound (Grasshoff, Ehrhardt and Kremling, 1983) (Detection limit: 0.3 μM).

CHAPTER FOUR
RESULTS AND DISCUSSION

4.1 Hydrography

4.1.1 Vertical Profiles

Before dealing with the chemical data from the Cilician Basin, we attempt to identify the hydrographic features in the water column. The composite depth profiles of potential temperature, salinity and sigma-theta (σ_θ) in the Cilician Basin, obtained during May 1997, July 1998 and October 2003 periods (Figure 4.1, 4.2 and 4.3).

The salinity profiles displayed an apparent seasonality. In spring, the surface mixed layer was separated from the deep water by a strong halocline, which was established at 25-50 m during May. The potential temperature profile shows the occurrence of the surface mixed layer with a temperature range of 19-22°C. The less saline deep waters (S ≅ 38.8 psu) were separated from an intermediate layer, which identifies LIW, extending down to 100-250 m with a temperature of about 16°C and constant salinity (S=39.2 psu).

In summer, the seasonal thermohaline feature formed below the mixed surface layer appeared at a depth of 50-75 m. Temperature was about 26-28°C at the surface and it decreased to 14°C below 250 m. Surface salinity increased (S=39.2-39.4 psu) due to surface heating and evaporation in this period. The occurrence of salty and warm surface waters in the Levantine Basin is the result of high rate of evaporation much exceeding fresh water input to the system (Ozsoy et al, 1989).

In fall, seasonal thermocline moved downward to 75-100 m and surface temperature starts to be cooling. The surface layer was occupied by more saline (S= 39.3-39.6 psu) and cooler (T= 24-26 °C) water than summer. During the summer and fall, the surface layer was separated from the less saline Atlantic origin waters (MAW) by a strong halocline.

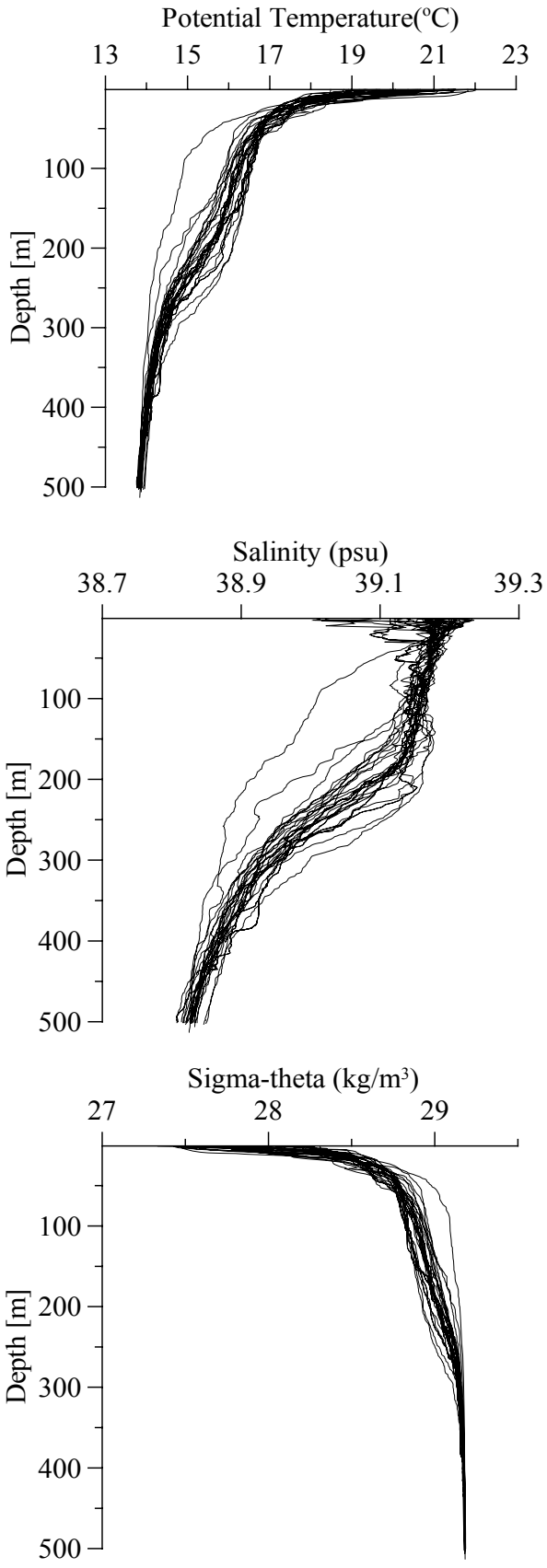

Figure 4.1 Vertical profiles in May 1997

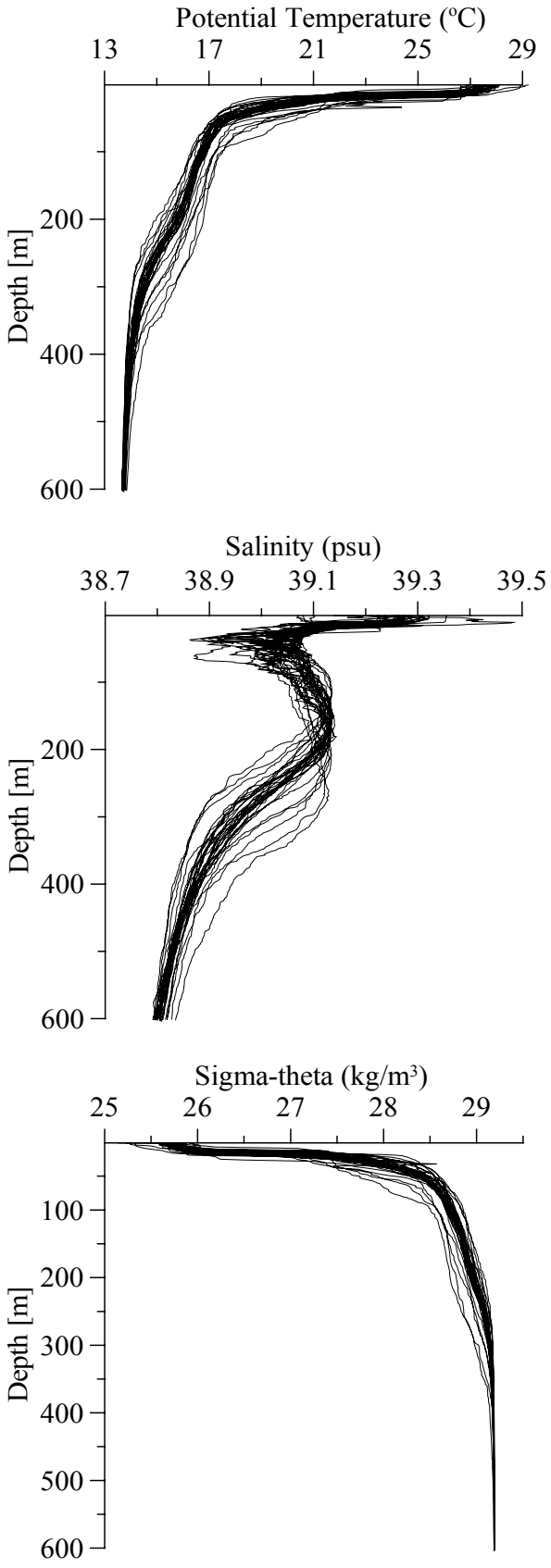

Figure 4.2 Vertical profiles in July 1998

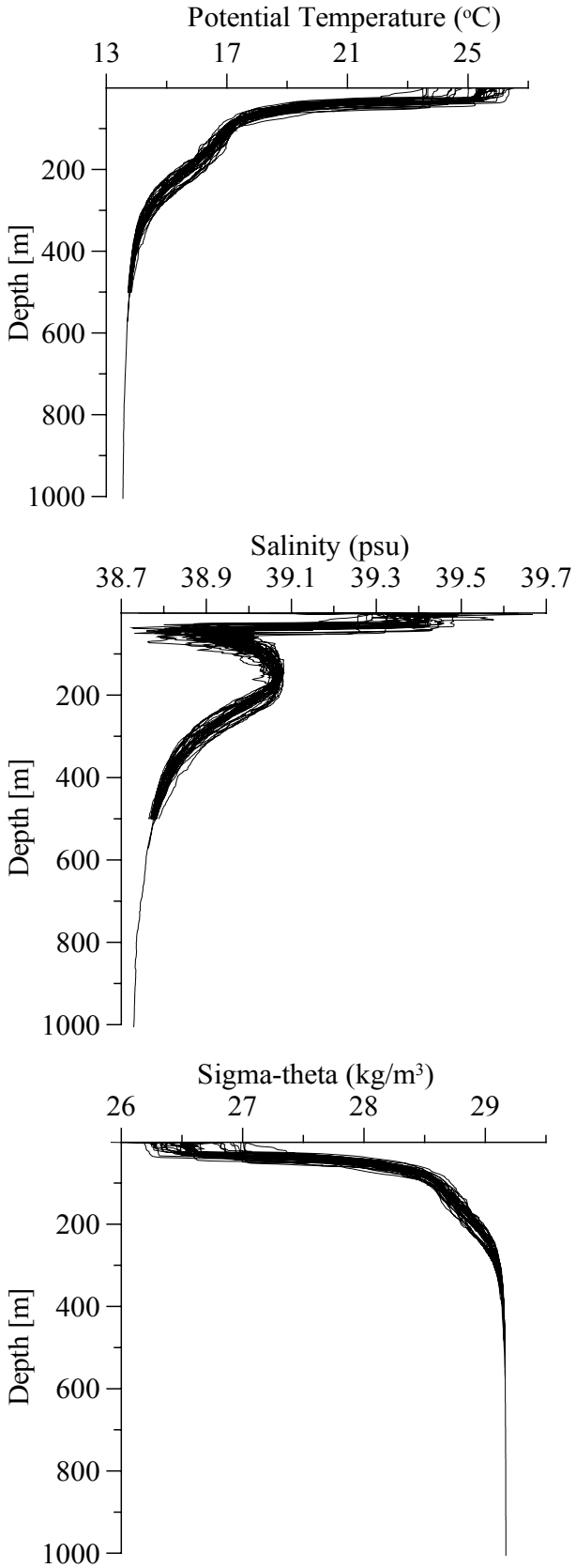

Figure 4.3 Vertical profiles in October 2003

The MAW was occupied by less saline (38.7-38.9 psu) and warmer (18°C) waters between 30 and 80 m than LIW (S=39.1-39.15, T=16-17°C) between 90 and 200 m. Combined data from several sampling points in summer, spring and fall cruises concluded that, the water properties were temperature 14˚C, salinity 38.7-38.8 psu and sigma theta 29.2 kg/m^3 below 300 m.

4.1.2 T-S Analysis of the Cilician Basin

To define the water mass properties and their major transformations during three surveys, we present potential temperature/salinity diagrams constructed for the Northern Cyprus (Figure 4.4, 4.5 and 4.6).

Figure 4.4 represents the composite θ-S diagram of all stations in May 1997 and clearly demonstrates the presence of the following indigenous and transit water masses: (1) Levantine Surface Water (LSW) of high salinity (39.2 psu), (2) Subsurface Levantine Intermediate Water (LIW) of salinity maximum (39.2 psu) and (3) Transitional Mediterranean Water (TMW) of low salinity (38.8 psu). The LIW is consistently detected in the θ-S diagram, i.e., the collection of data points with $S \geq 39.1$ psu, $\theta \cong 16$°C, and $\sigma_\theta \cong 28.9$ kg/m^3 in May 1997 (Figure 4.4)**.** After the period of intense winter convective mixing, there is evidence of spring warming at the surface re-stratifying the upper water column and resulting in the appearance of MAW. However during this period, the MAW is hardly discernible as a subsurface salinity minimum, probably due to mixing processes.

Throughout July 1998, surface salinities progressively increased (S = 39.2-39.4 psu) as a result of evaporation (Figure 4.5), and surface temperature became very high and exceeds 26°C. Subsurface MAW with salinity 38.9 psu and potential density (σ_θ) 28.3 kg/m^3 is located above a more saline and warmer LIW layer displaying similar characteristics ($S \cong 39.15$ psu, $\theta \cong 16$°C, and $\sigma_\theta \cong 28.9$ kg/m^3) with the preceding period.

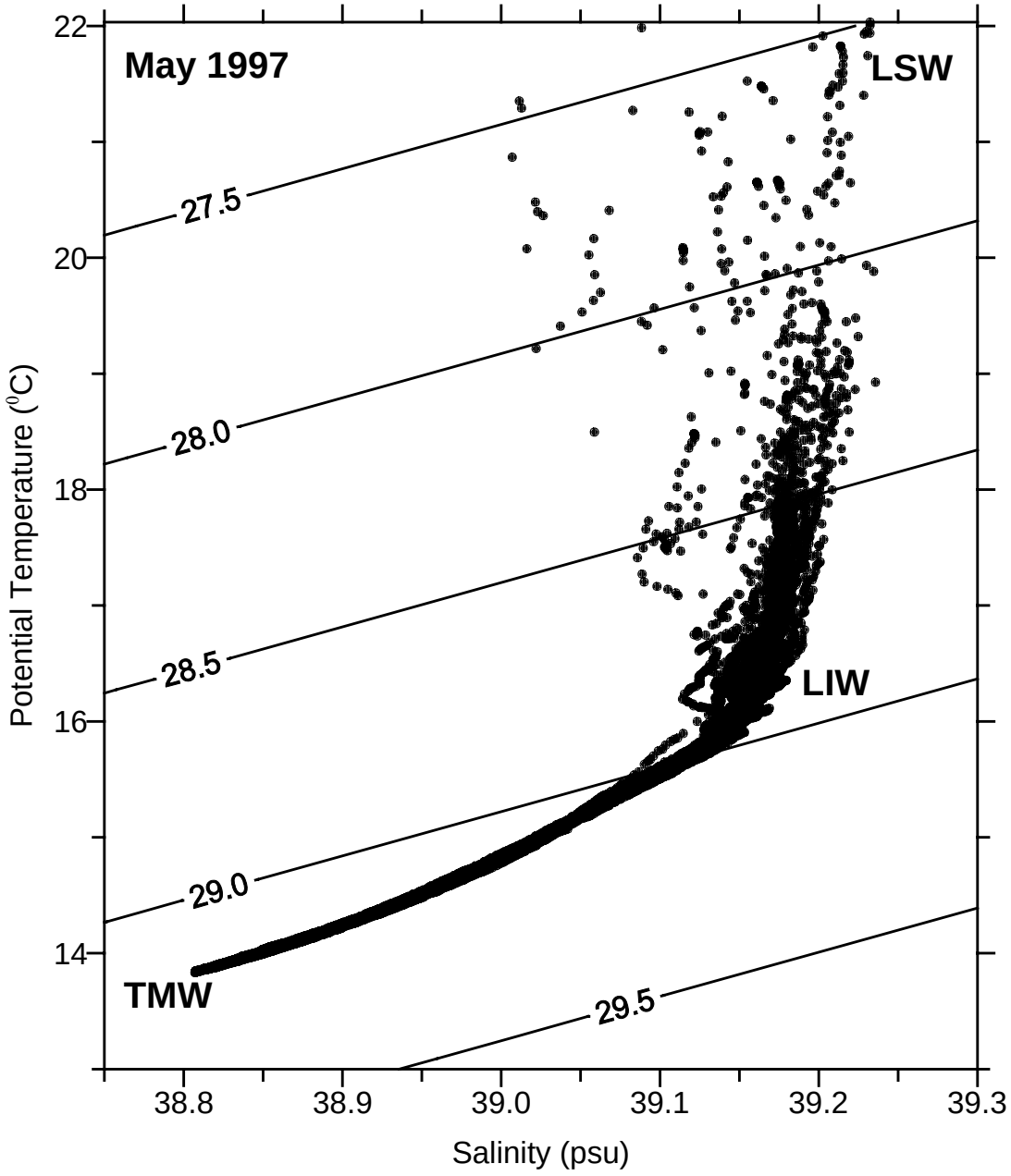

Figure 4.4 Potential temperature-salinity relationship in the Cilician Basin in May 1997

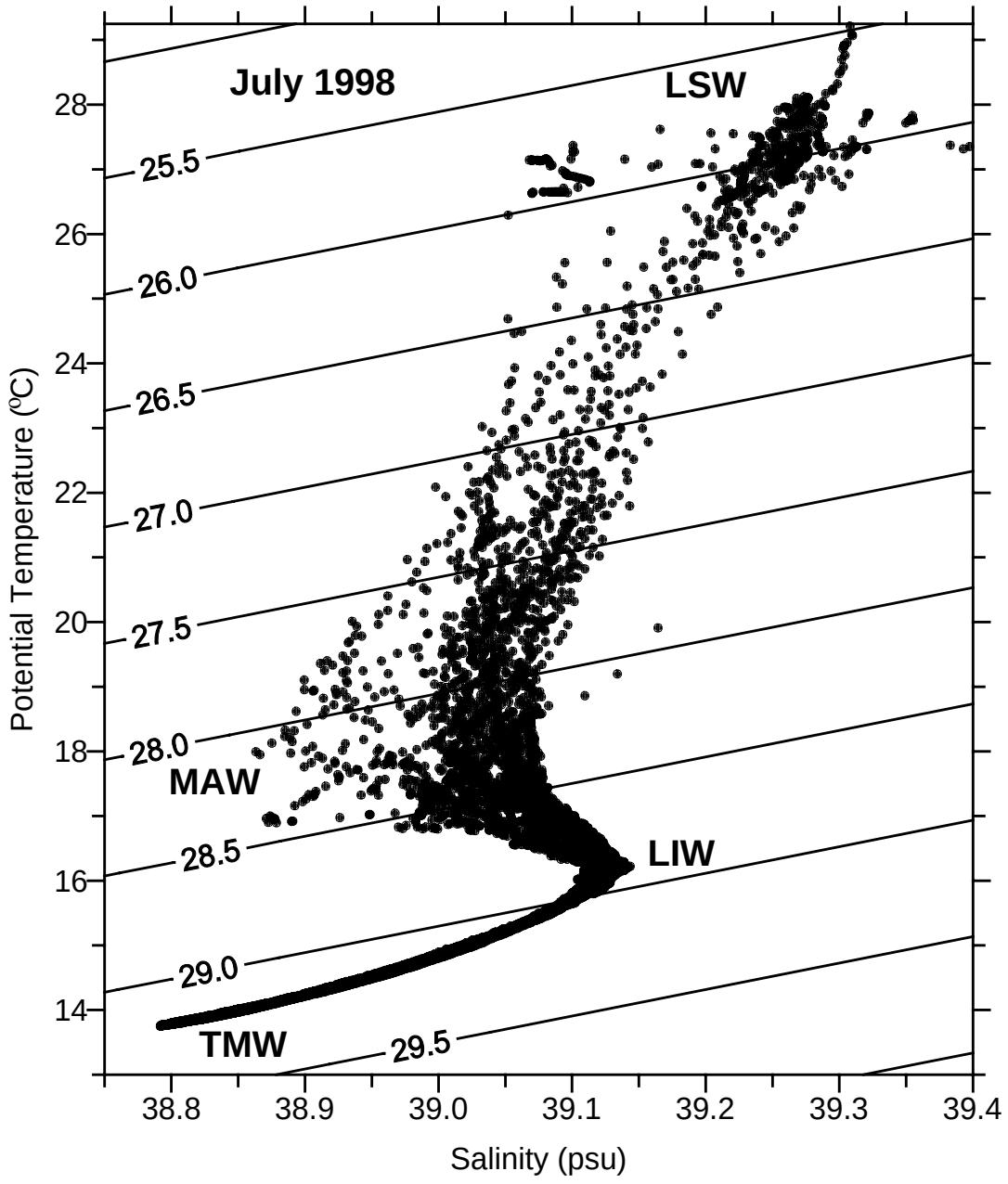

Figure 4.5 Potential temperature-salinity relationship in the Cilician Basin in July 1998

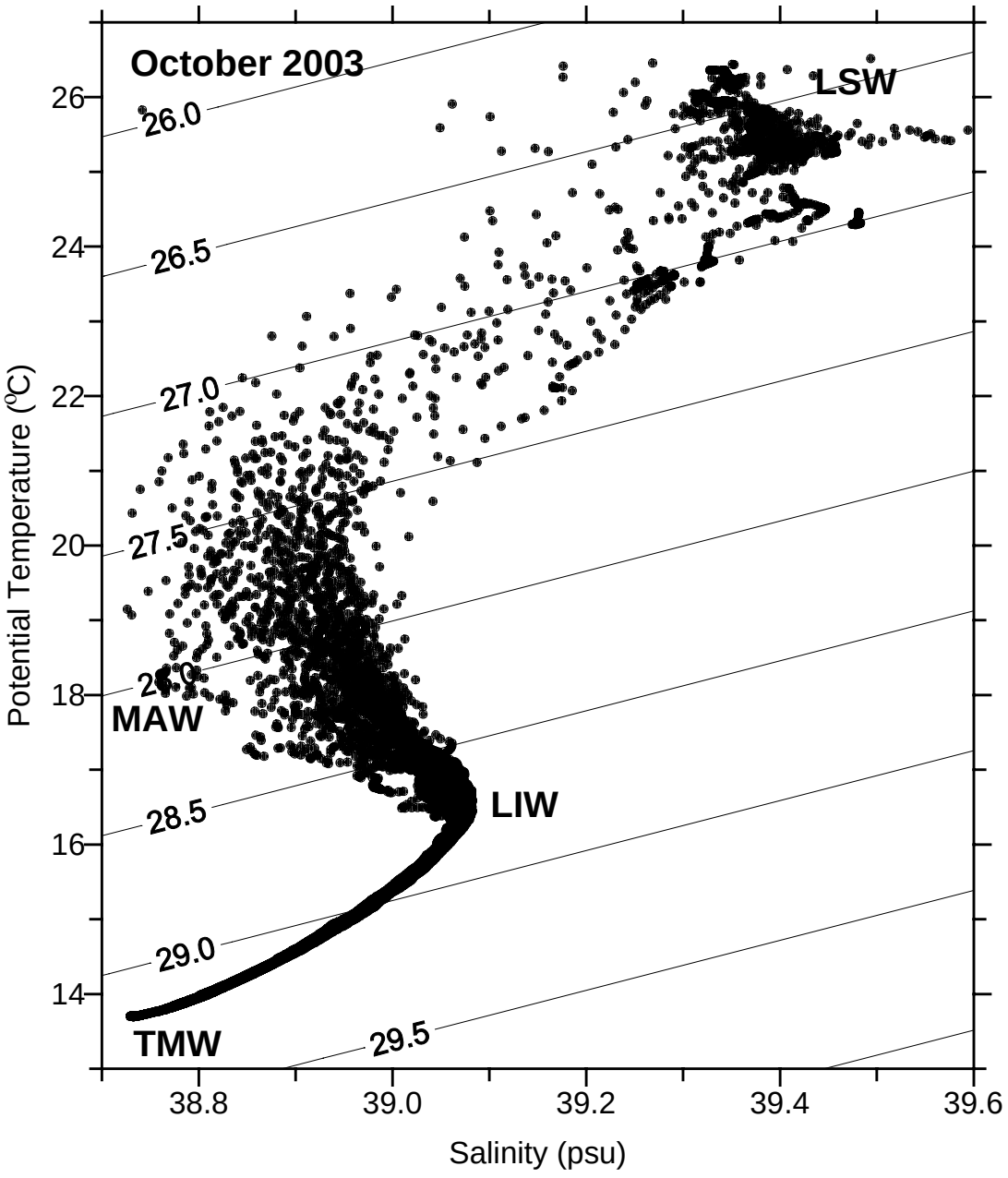

Figure 4.6 Potential temperature-salinity relationship in the Cilician Basin in October 2003

In the third period, October 2003, the composite θ-S diagram, (Figure 4.6), also reveals the presence of the four water masses: LSW, MAW, LIW and TMW, as identified in summer 1998. The surface layer was relatively cooler (between 24 and 26°C) and more saline (S = 39.3-39.6 psu) than July 1998, and initially the LIW has a salinity of about 39.1 psu in the potential density range $\sigma_\theta \cong 28.8$ kg/m^3. TMW are constant in all cruises with the characteristic of $\theta \cong 14$°C, $\sigma_\theta \cong 29.2$ kg/m^3.

Table 4.1 Water masses characteristics

Date		**LSW**	**MAW**	**LIW**	**TMW**
May 1997	θ (°C)	19-22	-	16	14
	S (psu)	39.2	-	39.2	38.8
	σ_θ (kg/m^3)	27.6	-	28.9	29.2
July 1998	θ (°C)	26-28	18	16	14
	S (psu)	39.2-39.4	38.9	39.15	38.8
	σ_θ (kg/m^3)	25.5-26	28.3	28.9	29.2
October 2003	θ (°C)	24-26	18	17	14
	S (psu)	39.3-39.6	38.7	39.1	38.7
	σ_θ (kg/m^3)	26.2-27.0	27.8	28.8	29.2

4.1.3 Statistical θ-S Analysis

Statistical analysis of T-S relations (interval of temperature 1°C, of salinity 0.01 psu) applied on data set for determining portion of water masses. Potential temperature was taken as the temperature. The frequency in spring, temperature values between 13.5-14.5°C at simultaneous salinity values of between 38.85 and 39.00 psu amounts, as may be seen from Figure 4.7, to 6751. This frequency covers 52.91% (the sum of the numbers are 12759) of all cases and represents TMW. LIW (T=15.5-16.0°C and S=39.1-39.2 psu) that has the frequency of 5822 covers 45.63% of all observations. MAW is hardly discernible in this month. θ-S relations on the surface indicate that 1.48% of all observations (frequency: 186) is LSW.

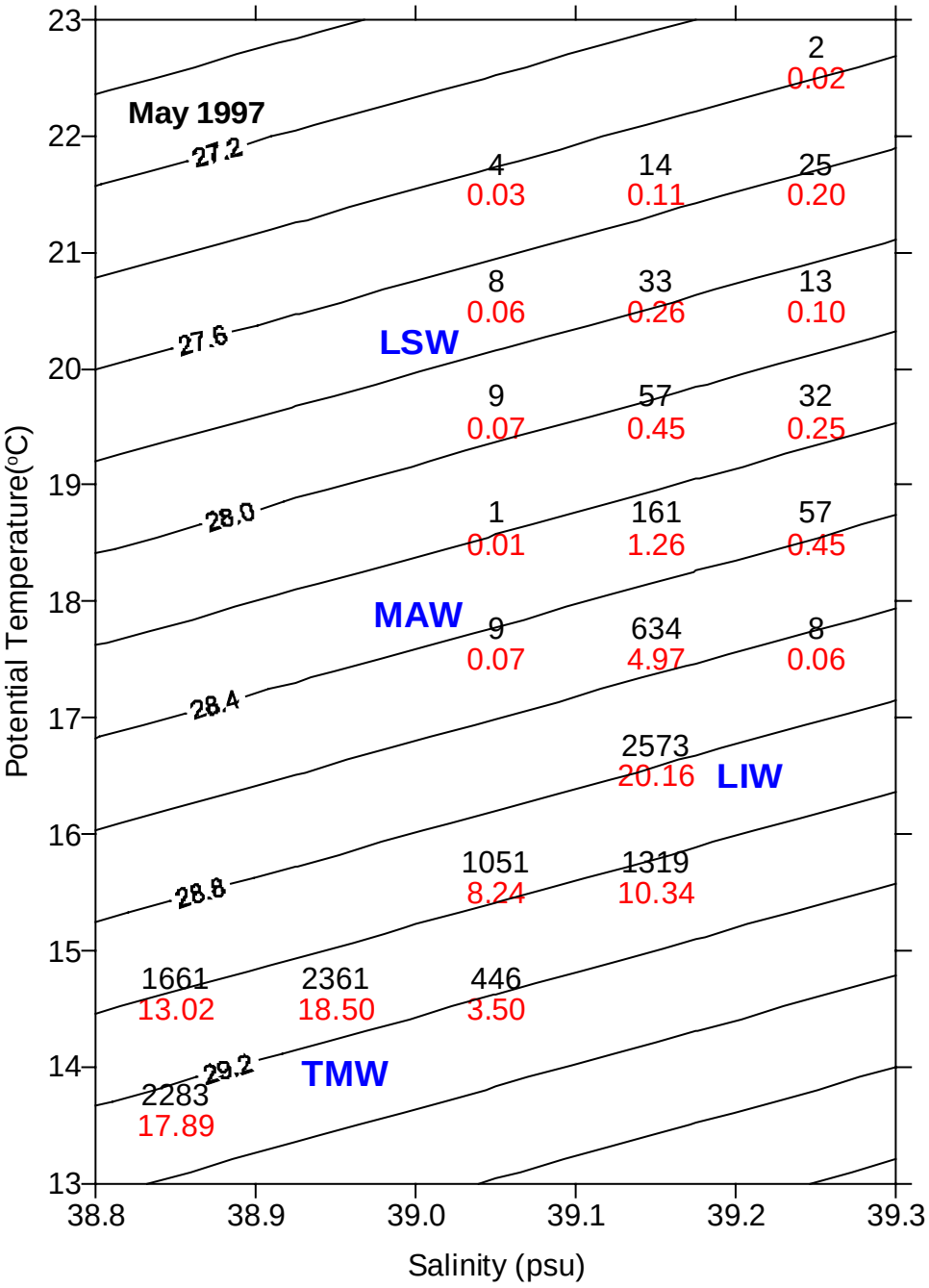

Figure 4.7 Statistical θ-S Analysis in the Cilician Basin in May 1997

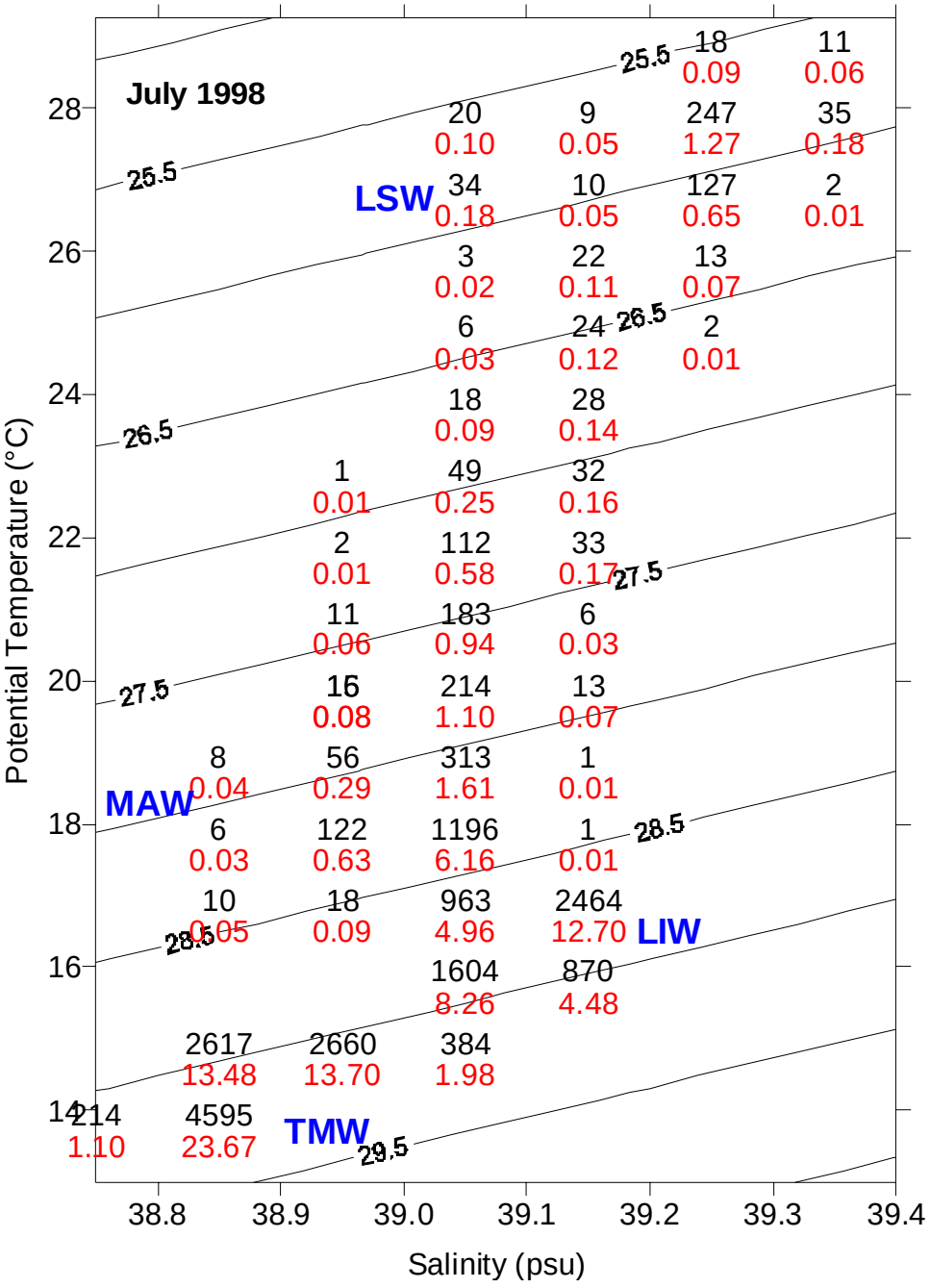

Figure 4.8 Statistical θ-S Analysis in the Cilician Basin in July 1998

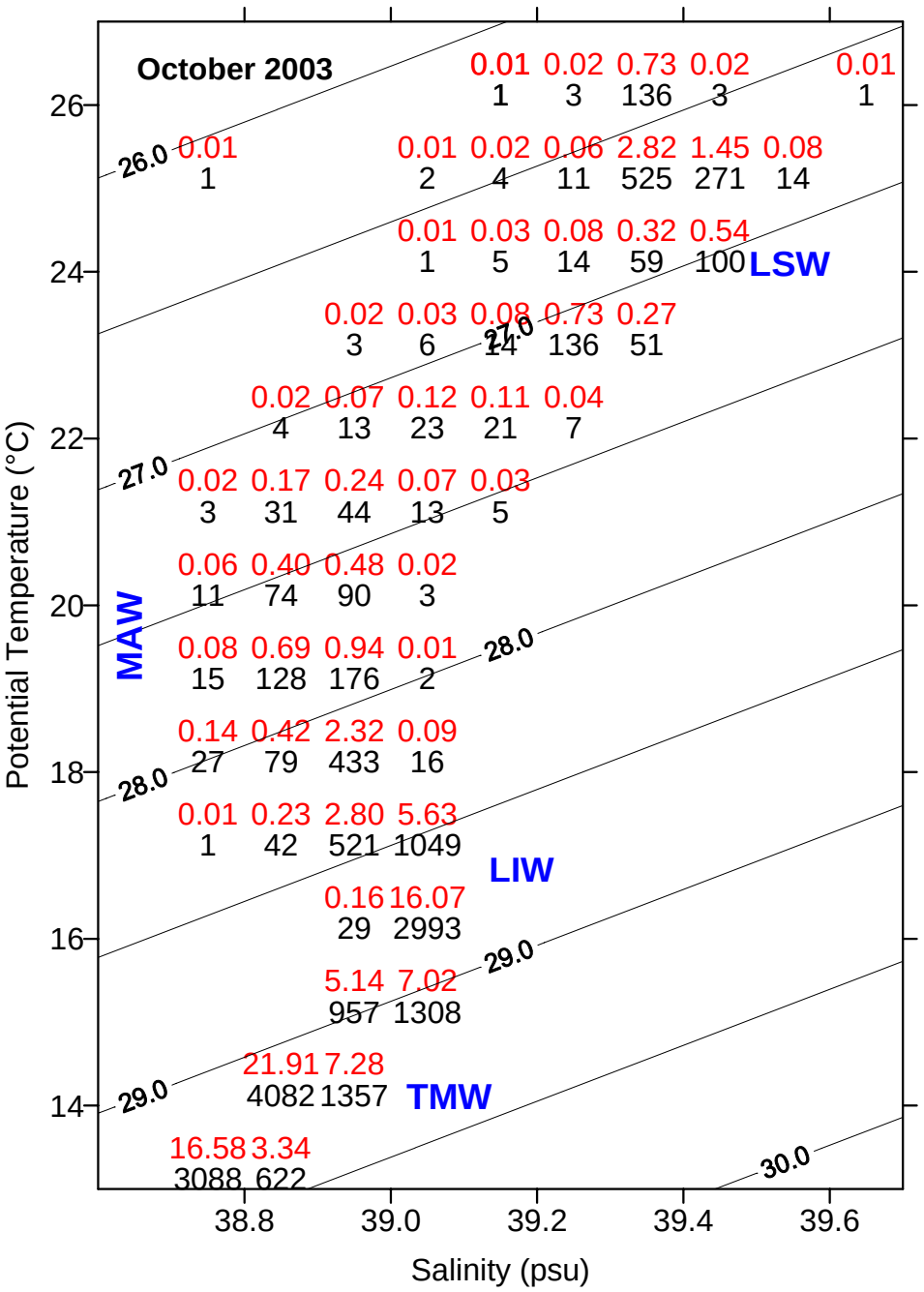

Figure 4.9 Statistical θ-S Analysis in the Cilician Basin in October 2003

The characteristics of statistical θ-S diagram in summer, is similar to the θ-S diagram given for spring. 52.83% of the volume of the waters (frequency: 10296) is TMW, which have same properties with spring. LIW and MAW exist 30.4% and 10.17% of the total volume, respectively. 5.44% of all observations are determined LSW, which is comprised between 24°C and 29°C. The total volume of LSW increases in summer, because the seasonal thermocline appeared at a depth of 50-75 m (Figure 4.8).

In fall, θ-S relations in the deep layer indicate that 49.15% of total observations is TMW (frequency is 6271). LIW, which displays similar characteristics to the preceding periods, covers 28.39% of total observations. MAW is characterized by minimum salinity (~38.9) psu in the fall like summer. MAW's frequency is 1894 and covers 14.85% of total observations. The volume of LSW increases and reaches 7.69% (frequency; 981) of all observations, because seasonal thermocline moved downward to 75-100 m (Figure 4.9).

4.1.4 The Basin Circulation and Its Variability

4.1.4.1 Dynamic Height Anomaly

Defant's ideas have been applied to the relative distribution of ΔD_A-ΔD_B as a function of depth for "Northern Cyprus" stations for three seasons in Tablo 4.2, 4.3 and 4.4. Figure 4.10 shows the values of ΔD_A-ΔD_B versus depth on the x axis. It is obvious that the most reasonable assumption of selecting the absolute zero for the differences of the anomalies of the dynamic depths of isobaric surfaces is placed around 400-500m. If the absolute zero for the differences of anomalies of the dynamic depths of isobaric surfaces is placed around 400-500 m, the proper direction of current will be obtained in the upper layer. The relative current at 400-500m depths is most likely to equal zero. Selected stations have different physical characteristics due to determining reference level. These are stations; 36-5, 36-1 for May 1997, stations; 1-34, 3-11 for July 1997 and stations; 3-37, 34-20 for October 2003.

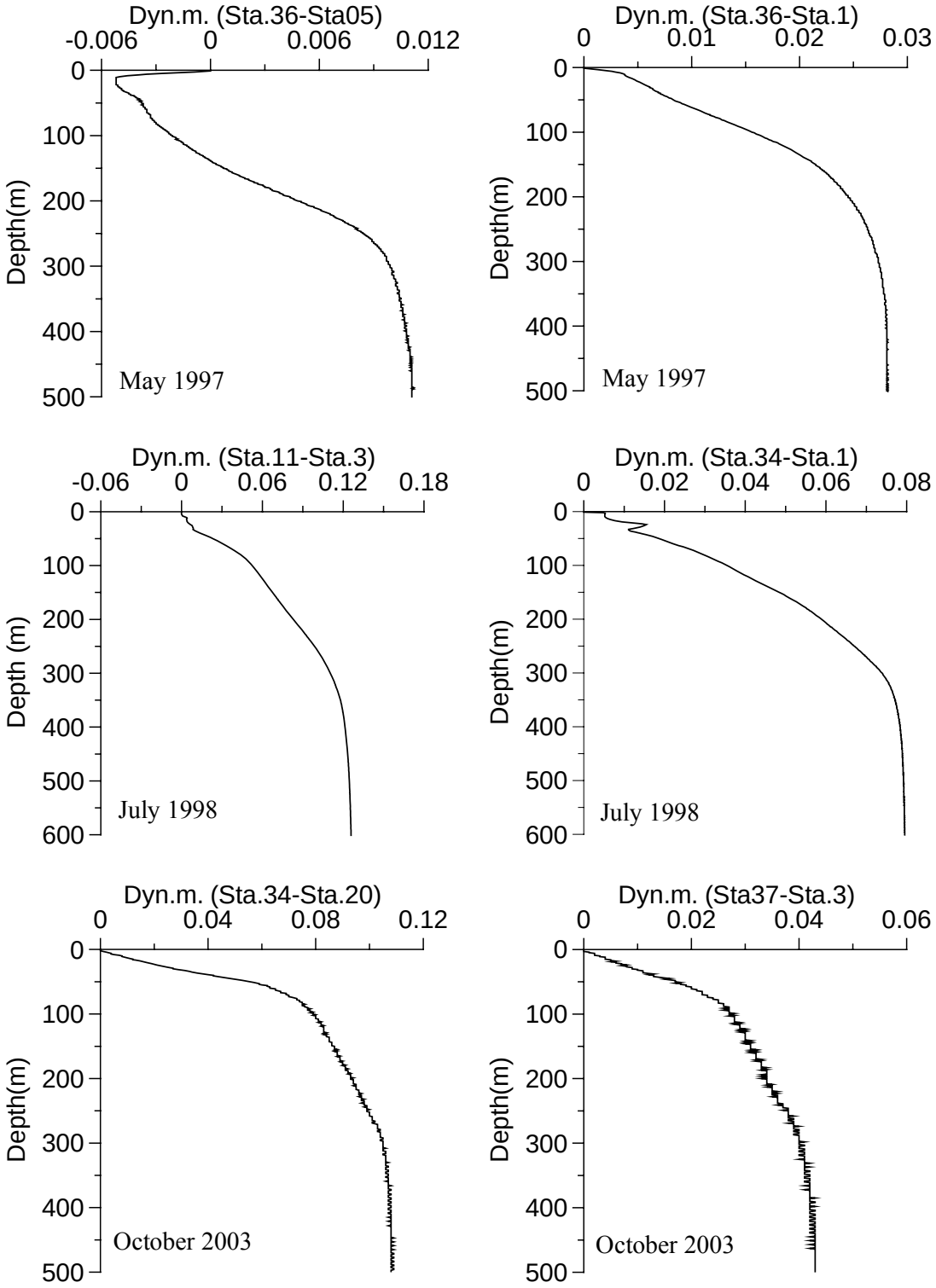

Figure 4.10 Dynamic depth differences between selected "Northern Cyprus" stations for all cruises (Defant's approach)

Table 4.2 Dynamic depth differences between selected "Northern Cyprus" stations in cruise, May 1997.

Depth (m)	ΔD_A (Dyn.m)	ΔD_B (Dyn.m)	ΔD_A-ΔD_B
	ΔD_{36}	**ΔD_5**	**ΔD_{36}-ΔD_5**
0	0	0	0
50	-0.0172	-0.021	0.0038
100	-0.0535	-0.0556	0.0021
200	-0.1355	-0.1307	-0.0048
300	-0.2245	-0.2146	-0.0099
400	-0.3134	-0.3026	-0.0108
450	-0.3571	-0.346	-0.0111
500	-0.4	-0.3889	-0.0111
	ΔD_{36}	**ΔD_1**	**ΔD_{36}-ΔD_1**
0	0	0	0
50	-0.017	-0.0255	0.0083
100	-0.054	-0.0691	0.0156
200	-0.136	-0.16	0.0245
300	-0.225	-0.2518	0.0273
400	-0.313	-0.3415	0.0281
450	-0.357	-0.3852	0.0281
500	-0.4	-0.4281	0.0281

Table 4.3 Dynamic depth differences between selected "Northern Cyprus" stations in cruise, July 1998

Depth (m)	ΔD_A (Dyn.m)	ΔD_B (Dyn.m)	ΔD_A-ΔD_B
	ΔD_1	**ΔD_{34}**	**ΔD_1-ΔD_{34}**
0	0	0	0
50	0.056	0.0373	0.0187
100	0.0485	0.013	0.0355
200	0.0011	-0.0578	0.0589
300	-0.07	-0.1434	0.0739
400	-0.154	-0.2319	0.0784
450	-0.197	-0.2756	0.0790
500	-0.239	-0.3186	0.0792
	ΔD_3	**ΔD_{11}**	**$\Delta D_3\Delta D_{11}$**
0	0	0	0
50	0.0375	0.0143	0.0232
100	0.0375	-0.0148	0.0523
200	-0.007	-0.0901	0.083
300	-0.068	-0.1783	0.1105
400	-0.147	-0.2684	0.1214
450	-0.189	-0.3125	0.1233
500	-0.231	-0.3559	0.1245

Table 4.4 Dynamic depth differences between selected "Northern Cyprus" stations in cruise, October 2003

Depth (m)	ΔD_A (Dyn.m)	ΔD_B (Dyn.m)	ΔD_A-ΔD_B
	ΔD_3	**ΔD_{37}**	**ΔD_3-ΔD_{37}**
0	0	0	0
50	0.062	0.079	0.017
100	0.051	0.078	0.027
200	-0.004	0.029	0.033
300	-0.082	-0.042	0.040
400	-0.167	-0.125	0.042
450	-0.210	-0.167	0.043
500	-0.250	-0.207	0.043
	ΔD_{34}	**ΔD_{20}**	**ΔD_{34}-ΔD_{20}**
0	0	0	0
50	0.084	0.028	0.056
100	0.091	0.012	0.079
200	0.047	-0.046	0.093
300	-0.023	-0.128	0.105
400	-0.106	-0.214	0.108
450	-0.148	-0.256	0.108
500	-0.189	-0.297	0.108

When we calculated the value of ΔD_A-ΔD_B, we could equally well have deduced that the difference in the dynamic height of isobar *p1* between stations A and B. Such variations in dynamic height are described as dynamic topography (The Oceanography Course Team, 1993). The dynamic height anomaly maps at the surface and 200 m depth relative to 450 m were given in Figure 4.11, 4.12 and 4.13. The contours were labeled in dynamic meters.

Geostrophic current were compute from dynamic topography with equation 7 and represented in the next section (The Basin Circulation and Its variability).

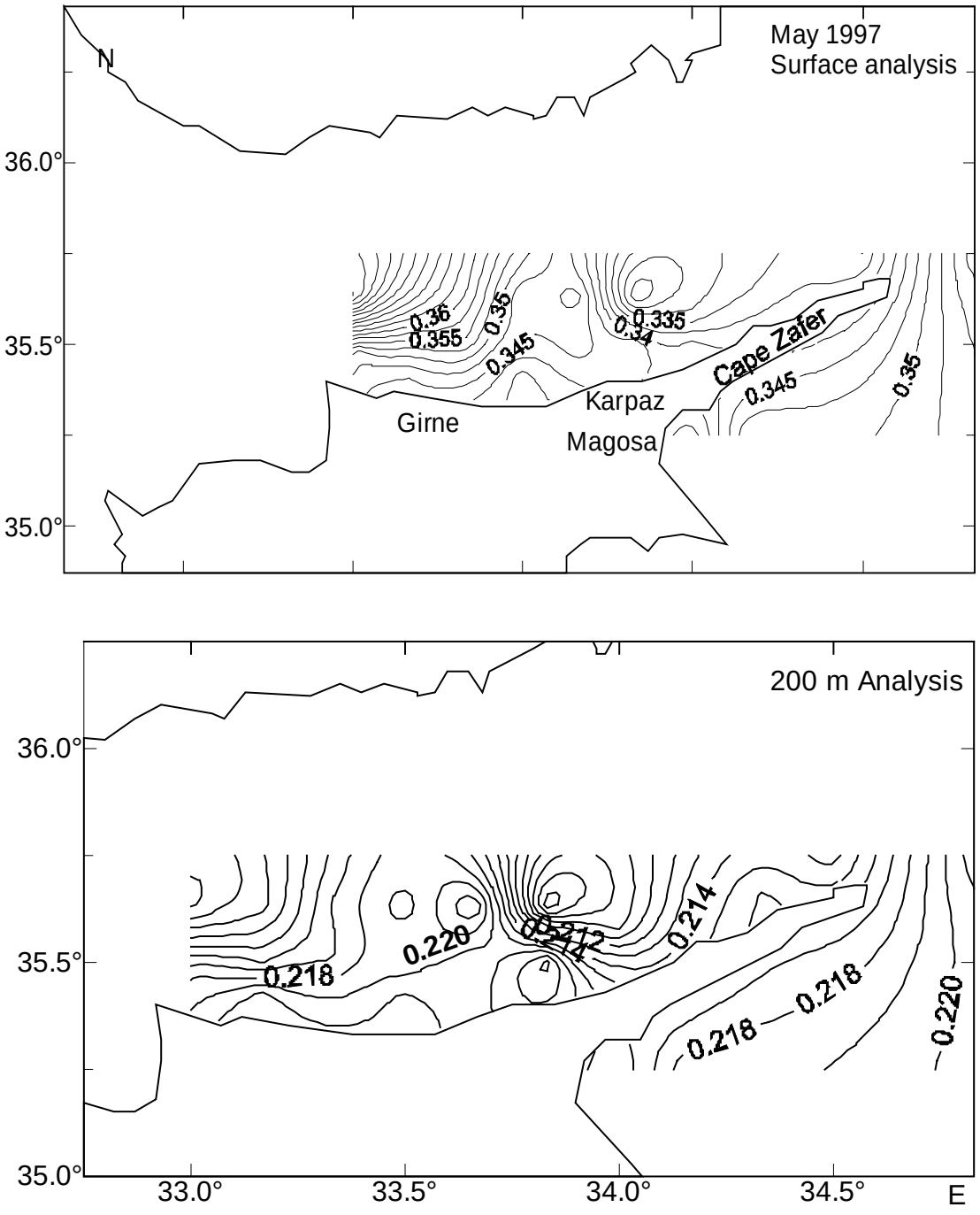

Figure 4.11 Dynamic height anomaly (m^2/s^2) at surface and 200 dbar with reference to 450 m in May 1997

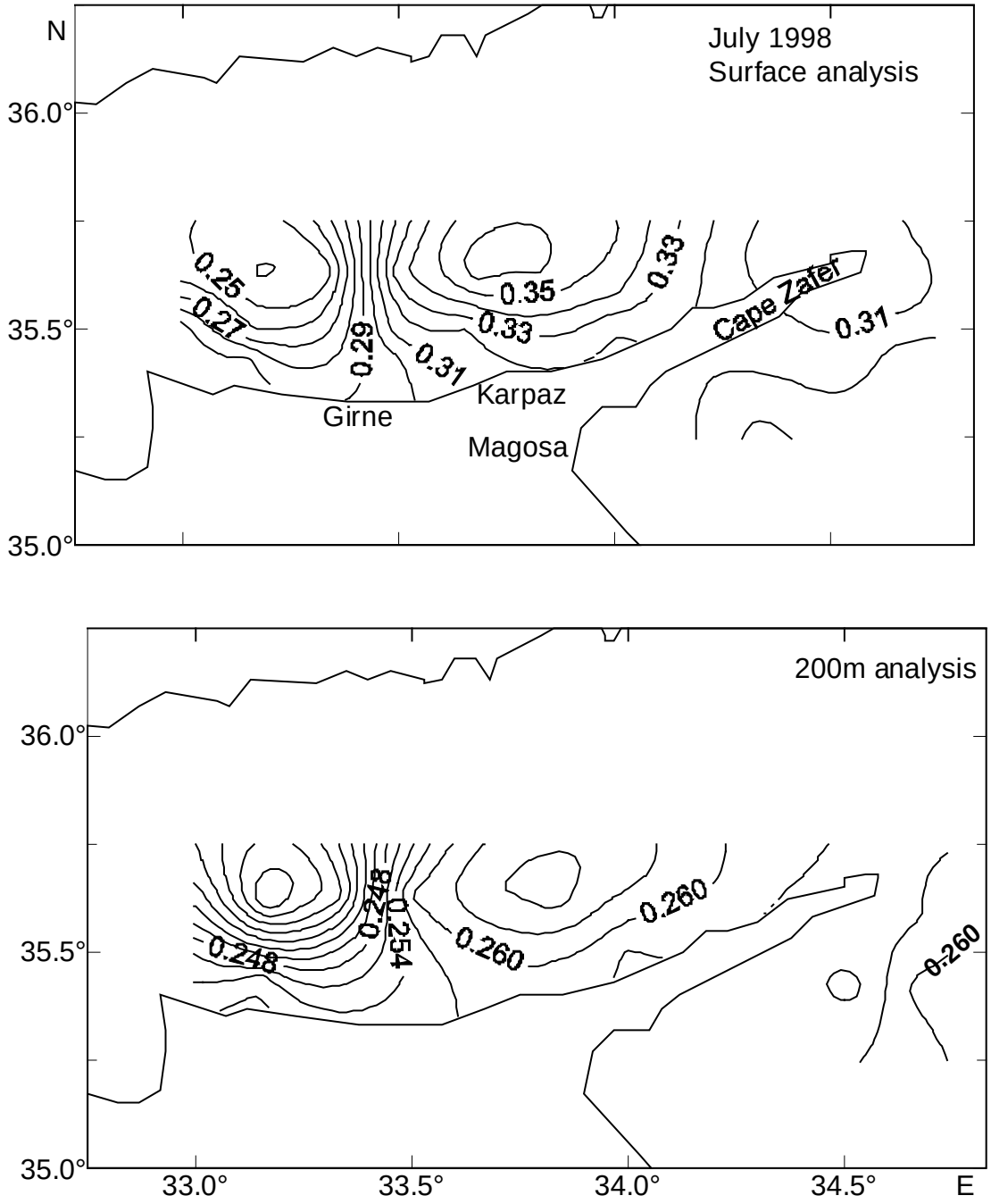

Figure 4.12 Dynamic height anomaly (m^2/s^2) at surface and 200 dbar with reference to 500 m in July 1998

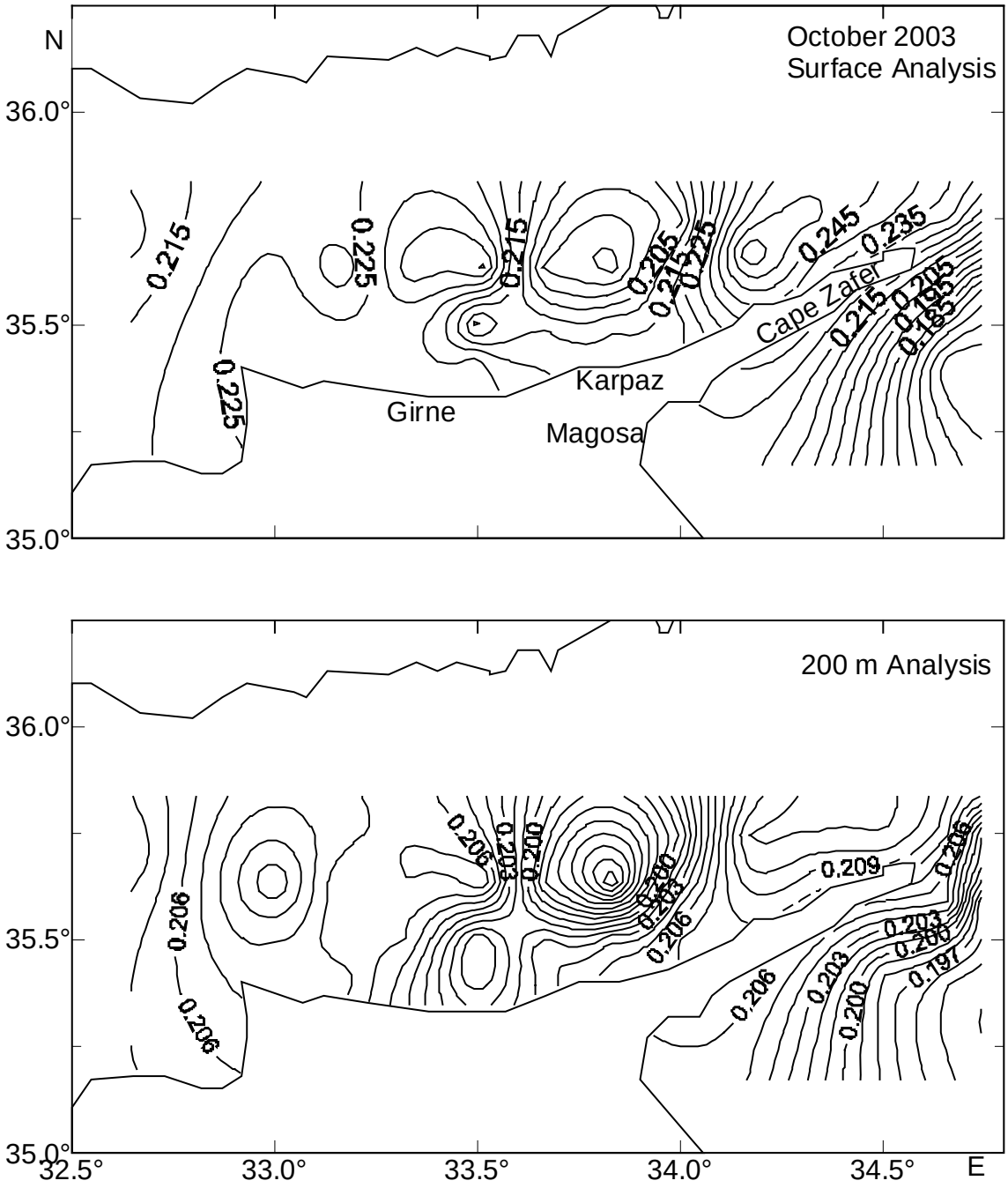

Figure 4.13 Dynamic height anomaly (m^2/s^2) at surface and 200 dbar with reference to 450 m in October 2003

4.1.4.2 The Basin Circulation and Its Variability

The first data set, obtained in May 1997, demonstrates the major elements; the shape, position, strength of gyres, strength and direction of currents of the Cilician Basin circulation (Figure 4.14) The current flows towards to the north along the eastern coast of Cyprus, on the western side of the Lattakia Basin. Upon leaving the Lattakia Basin, the direction of the flow is unclear due to inadequate sampling coverage in the Cilician Basin. The presence of a cyclonic eddy to the north of the Karpaz and an anticyclonic meander offshore of Girne further west indicates a large cyclonic meander of the flow within the eastern part of the Cilician Basin. The flow seems to first proceed northward and then to swing south around the cyclonic eddy. It is interesting to note that, Ozsoy et al. (1993) also observed two such small eddies in the Cilician Basin during June 1987. During May 1997 cruise the average speed of geostrophic current was calculated to be 15 cm/s and reached a maximum speed of 25 cm/s at the surface.

The circulation to the north of Cyprus in July 1998 is opposite of that observed at May 1997 (Figure 4.15). The flow proceeding northward along the east coast of Cyprus first meanders anticyclonically and then swings offshore within the central part of the Cilician Basin. This offshore flow is also supported by a cyclonic eddy situated further west. These eddies, whose influence extend to intermediate depth, constitutes the most intense (30-35 cm/s) and dominant dynamic feature in summer 1998. The estimated velocities are stronger than the flow activities in May 1997. The surface and intermediate circulation patterns are both similar to each other.

The regional flow system during October 2003 reveals significant changes with respect to the former patterns. The northward coastal flow in the Lattakia Basin has been replaced by a stronger southward current. Central Levantine Basin waters could not be observed in the Cilician Basin due to insufficient sampling coverage. The flow may possibly enter into the Cilician Basin along the Syrian coast (Figure 4.16).

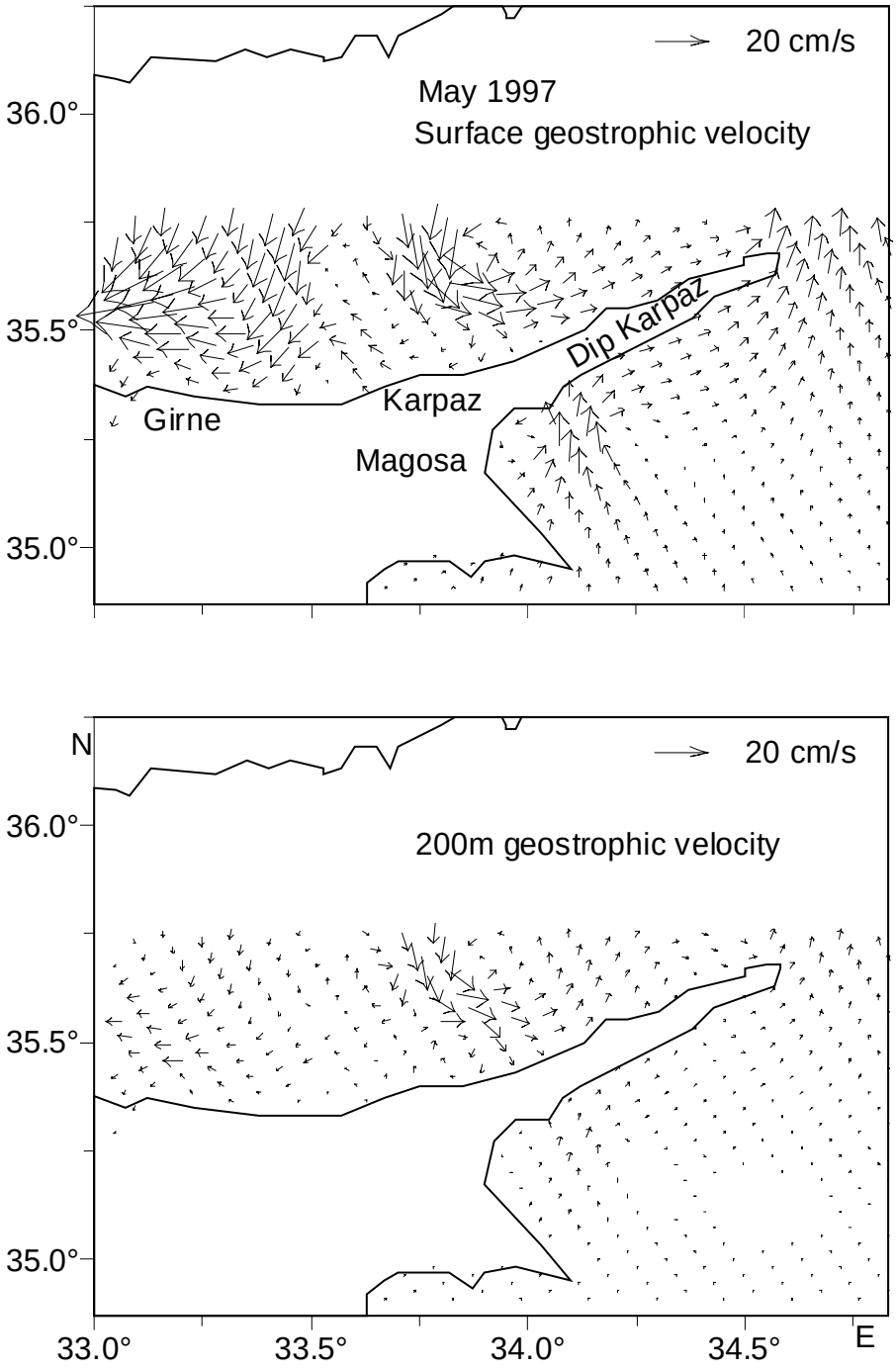

Figure 4.14 The geostrophic velocity structure at surface and 200m in units of cm/s for May 1997

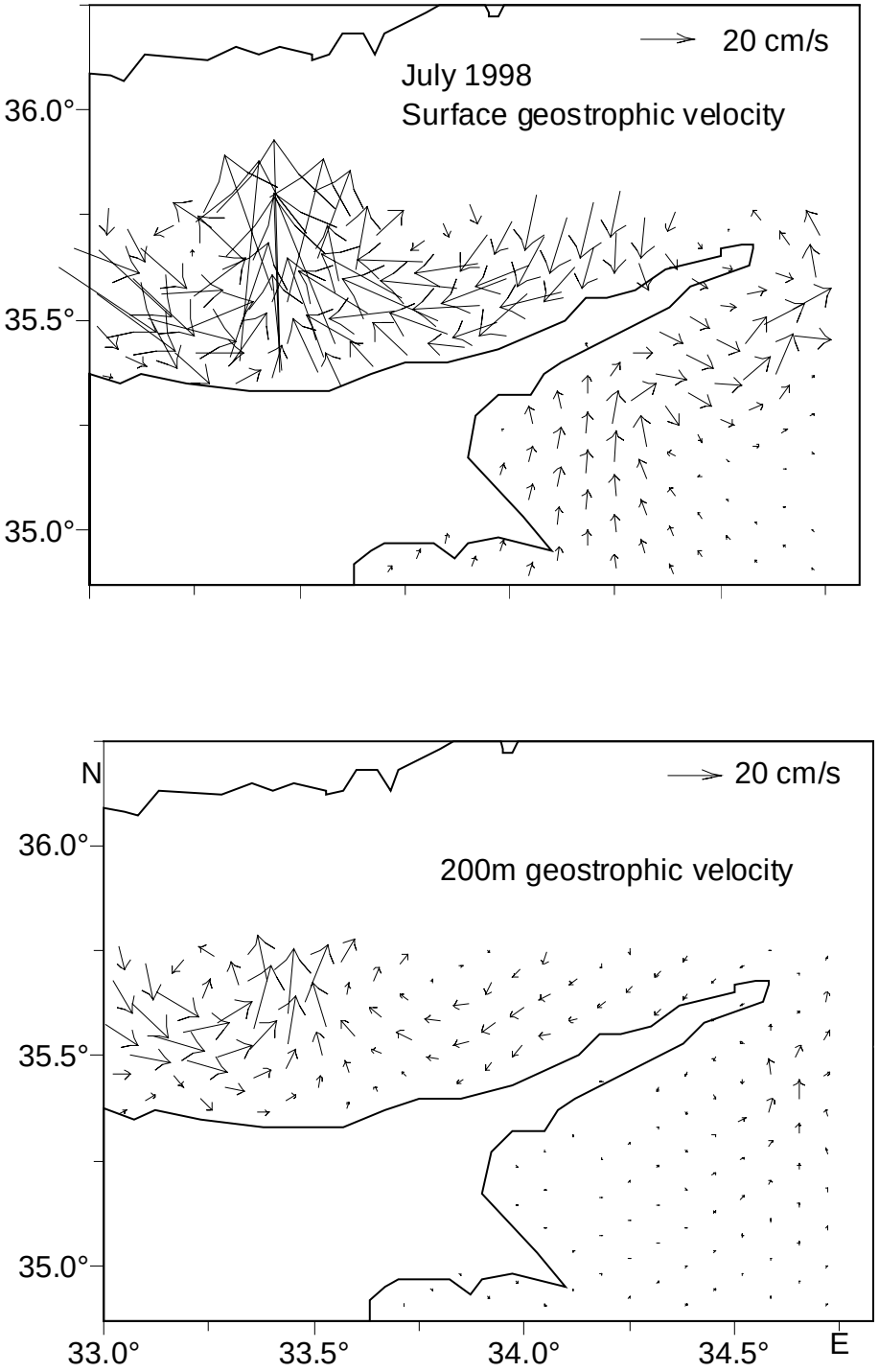

Figure 4.15 The geostrophic velocity structure at surface and 200m in units of cm/s for July 1998.

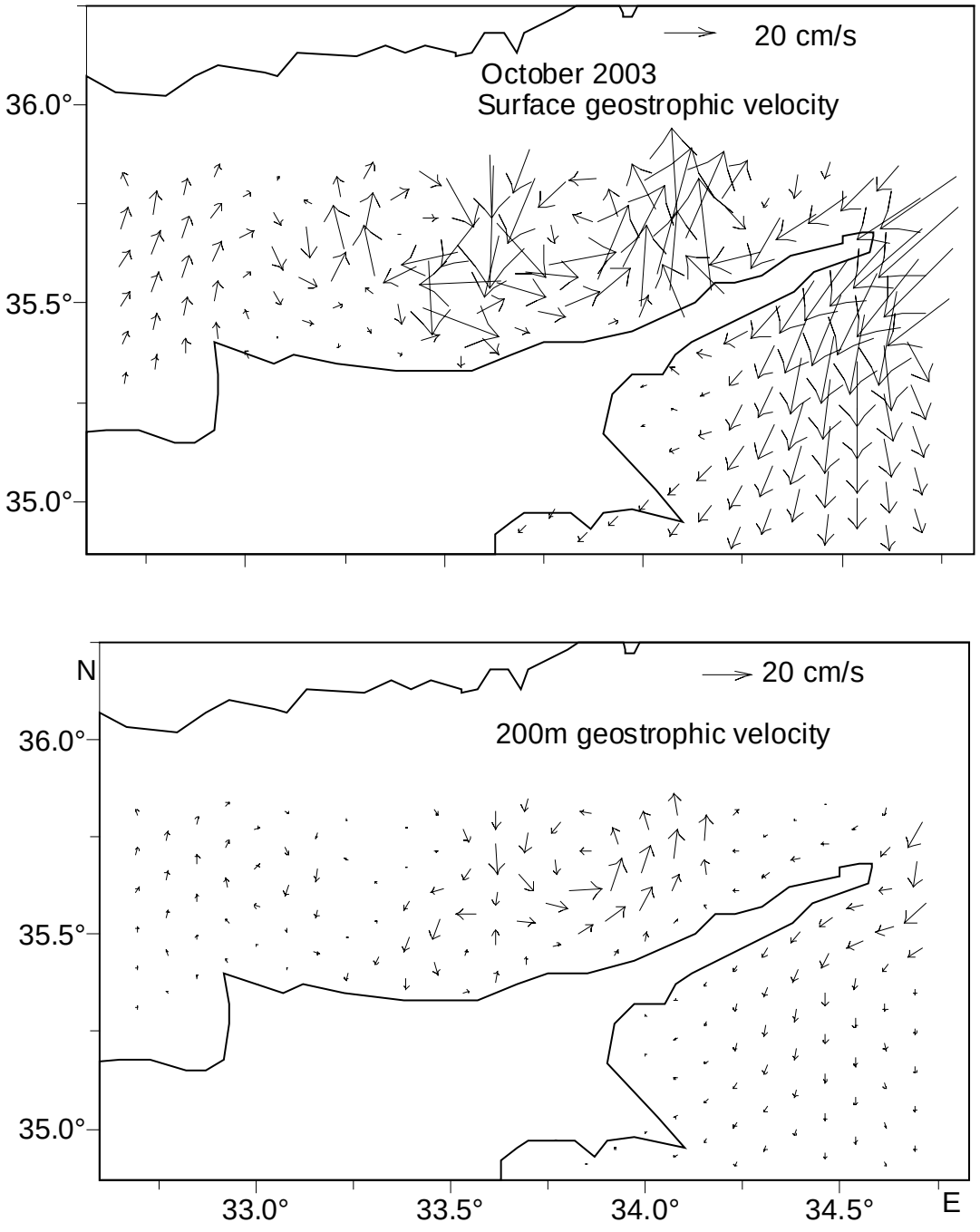

Figure 4.16 The geostrophic velocity structure at surface and 200m in units of cm/s for October 2003

The circulation to the north of Cyprus possesses a more disintegrated and patchy flow system formed by three adjacent small eddies. A cyclonic eddy is situated on the eastern side and is attached to an anticyclonic eddy in the middle and another anticyclonic eddy on the western side of the domain. The estimated velocities are 20-25 cm/s at the surface and rather weak (<10 cm/s) at 200 m depth (Figure 4.16). Robinson et al. (1991) and Ozsoy et al. (1993) found the similar results in October-November 1985 survey.

A final result is that many of persistent features found in the geostrophic circulation patterns can not be related to control exerted by the potential vorticity (f/H) upon the circulation (compare for instance, the patterns of Figure 4.14, 4.15, 4.16 with Figure 2.1 which shows the bottom topography). The flow structure reflects highly dynamic temporal variability in the system. The flow between the Lattakia and Cilician Basins along the Cyprus coast is prevented by Cape Zafer (the 'tip' of Cyprus) can be ascribed to the steep topography, associated with the sill between Cyprus and the Gulf of Iskenderun. At intermediate depths (200m) the flow patterns appear to be weakened (<5 cm/s) when compared to that of the surface.

Analysis of data collected during the multinational POEM programme (Brenner 1991; POEM Group, 1992; Robinson et al., 1987) has shown that the circulation in the Levantine Basin is composed of a complex series of sub-basin-scale gyres, jets and energetic mesoscale eddies. Similar conclusions were drawn by Hetch et al. (1988) based on data from the 17 Marine Climate cruises (MC) during the period 1979-1984. It is particularly worthwhile to compare our results with POEM data to detect whether any observable changes took place because there is significant time lag between these sampling. The circulation in May 1997 is very similar to those results from Eastern Mediterranean (Ozsoy et al., 1991, 1993). In July 1988 (POEM05), a branch of the Central Levantine Basin Current flows east, then north along the Syrian coast to feed the meandering Asia Minor Current (AMC) in the Cilician Basin (Ozsoy et al., 1991, 1993). In this study, the Central Levantine Basin Current was able to penetrate into the Cilician Basin through the eastern passage of Cyprus too. Nevertheless, AMC was not defined due to insufficient data set in this study. In August-September 1987 (POEM05), none of the Central Levantine Basin

Current waters seemed to penetrate into the Cilician Basin and the weak anticyclonic circulation persisted in the basin (Ozsoy et al., 1991, 1993; POEM Group, 1992; Robinson et al., 1991). The persistence of the basic circulation elements throughout the October 2003 indicates that the hydrographic regime was similar to the POEM05 observations. The circulation in October 1988, the main part of the flow passes east of Cyprus to join with the meandering jet in the Cilician Basin (Ozsoy et al., 1993). But the circulation pattern observed in October 2003 was significantly different from this observed in October 1988, suggesting interannual variability.

4.1.5 Advection of Atlantic Water Masses

The Atlantic Water (AW) enters the Levantine Basin through the Cretan Passage; it is then carried around by the jet flow with which is associated, and depending on the fate of the jet and entrainment into the various nearby eddies, it finds its way into the northern Levantine region in form of subsurface filaments (Ozsoy et al., 1989). A composite section across the basin from Girne to Dip Karpaz called VS1, an other section from Gazi Magosa to Dip Karpaz called VS2 were selected (Figure 4.17). The salinity distribution will be used for determining the Atlantic Water through the vertical sections. In each plot, the near surface (40-50 m) line contours with salinities of ≤38.9 psu were used to identify the AW masses. The water masses with AW signature (≤38.9 psu) were shaded in the figures.

In the May 1997 survey (Figure 4.18), the AW signature in the Cilician Basin is lost because of wintertime mixing. VS2 cross-section could not plot due to lack of data in May 1997.

An AW is found in the Cilician Basin in July 1998. There is also an AW trace at the easternmost station of the section, showing a partial penetration by way of the connection east of Cyprus. It is quite clear from the circulation derived from this summer survey that the circulations features have not changed significantly as compared with the May 1997 cruise. As a result of geostrophic circulation (Figure 4.19), AW could not reach to the Lattakia Basin.

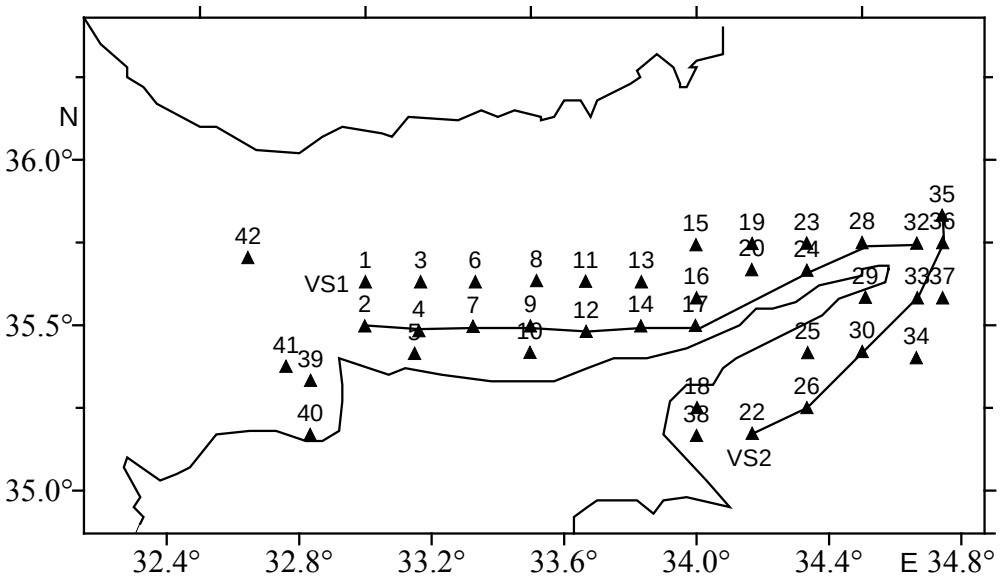

Figure 4.17 Locations of transects of stations for which the salinity distributions

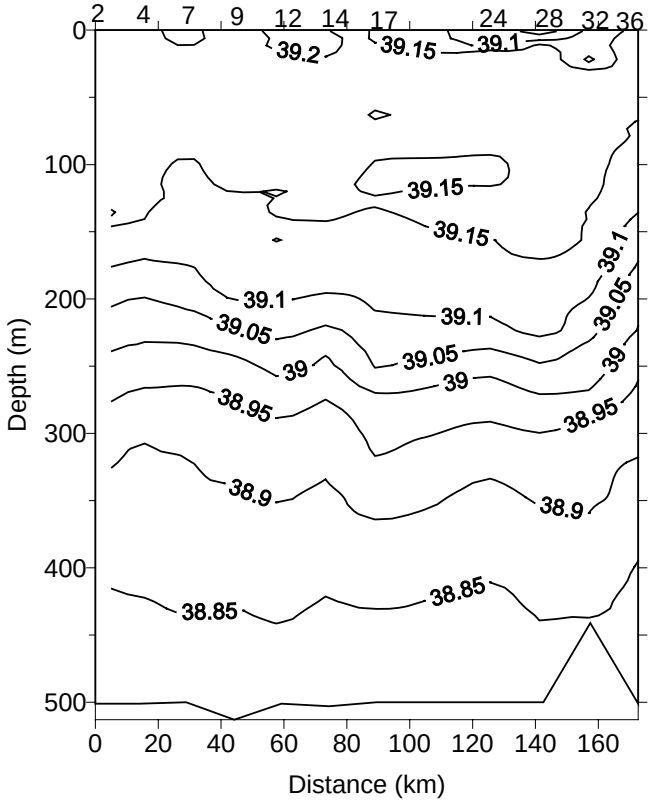

Figure 4.18 VS1 cross-section of salinity in May 1997 at the transect shown in Figure 4.17

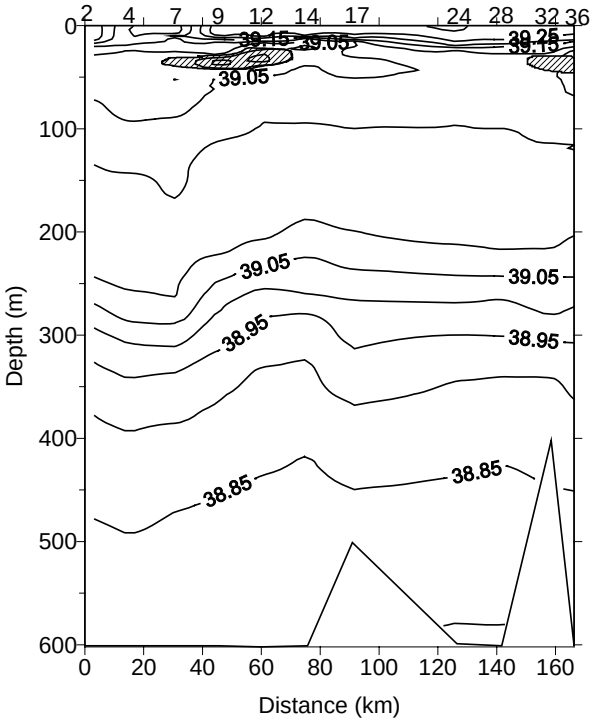

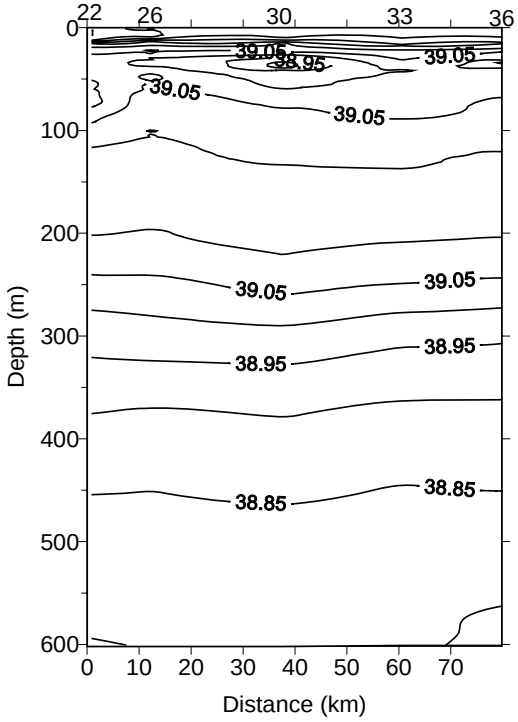

Figure 4.19 VS1 and VS2 cross-sections of salinity in July 1998 at the transects shown in Figure 4.17

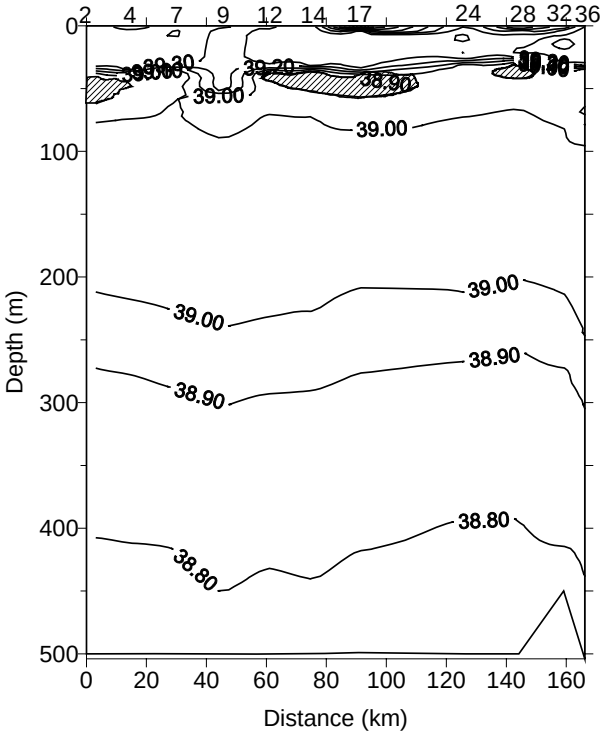

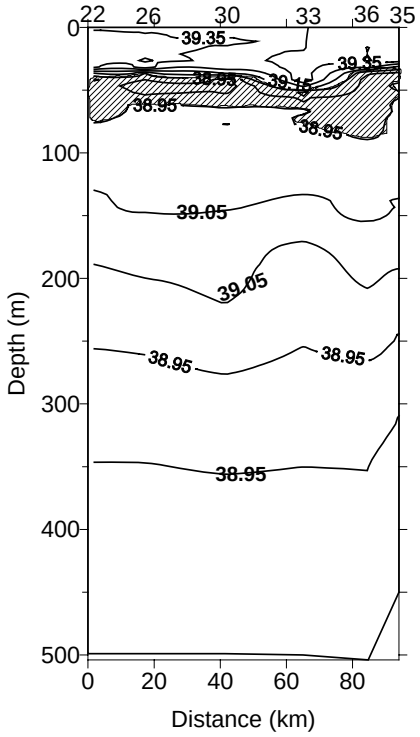

Figure 4.20 VS1 and VS2 cross-sections of salinity in October 2003 at the transects shown in Figure 4.17

It is only in October 2003 (Figure 4.20) that we see voluminous amounts of AW penetrating the region east of Cyprus. We observe a layer of AW extending at 40-50m. AW filament appears at the Lattakia Basin for the first time, suggesting some penetration of these waters from the Cilician Basin. The strong southward current at the east of Cyprus (Figure 4.20) carried the AW to the Lattakia Basin. AW enters the Latakia Basin due to the geostrophic circulation (Figure 4.16).

4.2 Nutrients

Nutrient concentrations measured in the water column of the Cilician Basin exhibited remarkable variations with depth, region and season. These samples were collected from surface to 500m during May 1997, October 2003 cruises, and from surface to 300m in July 1998. All the basin-wide nutrient data have been examined with respect to potential temperature, salinity and water density (sigma-theta). The composite profiles produced from the all data sets were illustrated in Figure 4.21-4.29. These vertical features would lead us to define both the boundaries of the hydro-chemically different water masses and the ranges of the nutrient concentrations in physically similar or different water masses. Salinity dependent nutrient profiles were used to define water masses because water masses with similar densities had seasonally varying salinities and temperatures.

The density dependent nutrient profiles clearly show that the nutrient-poor upper layer extends consistently down to the depths of the 29.0 kg/m^3 density surfaces in all three surveys with constant values in the upper layer of <0.02 μM phosphate, ~0.2 μM nitrate and 1 μM silicate (Figure 4.21, 4.24, 4.27). The lower nutrient concentrations appearing in the upper nutricline represent data from the less saline (38.7-38.8 psu) modified Atlantic waters (MAW) topping the more saline LIW (T=15.5-16°C and S=39.1-39.2 psu) during the October 2003 (Figure 4.22, 4.25, 4.28 and Figure 4.6).

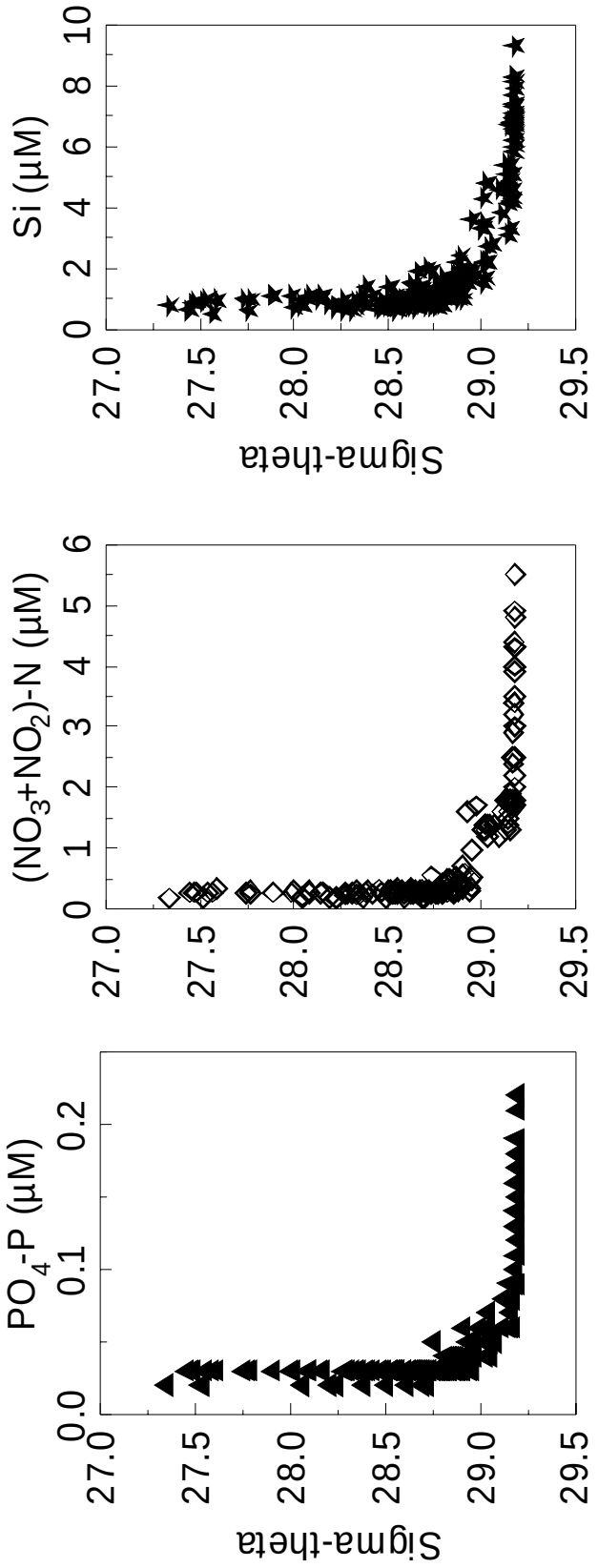

Figure 4.21 The plots of dissolved nutrients versus sigma-theta for the whole basin in May 1997

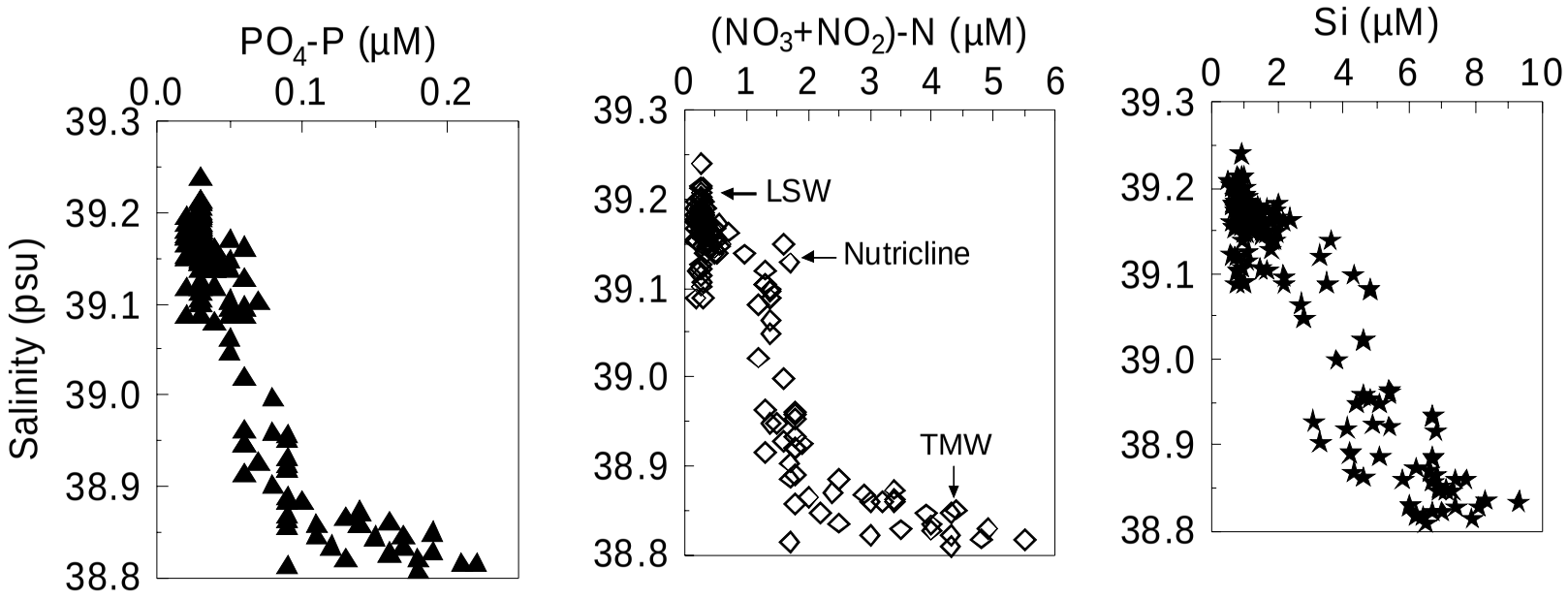

Figure 4.22 The plots of dissolved nutrients versus salinity for the whole basin in May 1997

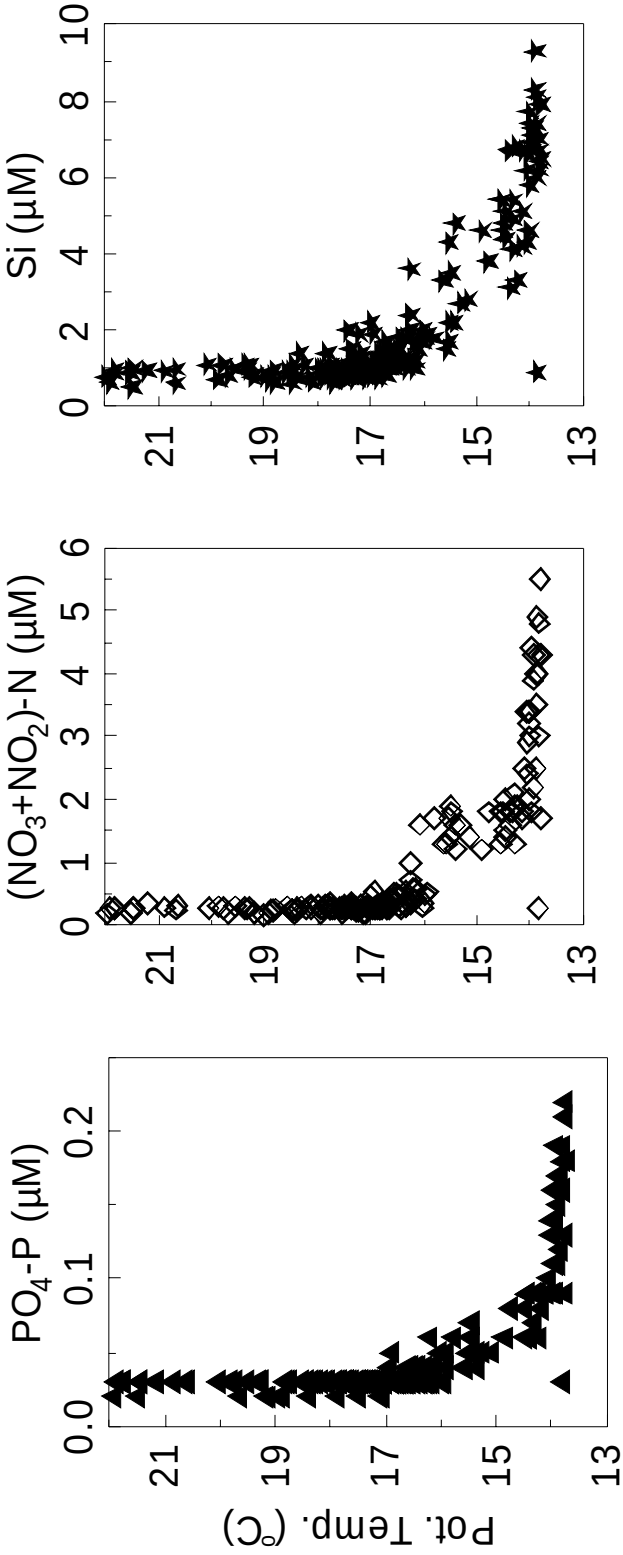

Figure 4.23 The plots of dissolved nutrients versus potential temperature for the whole basin in May 1997

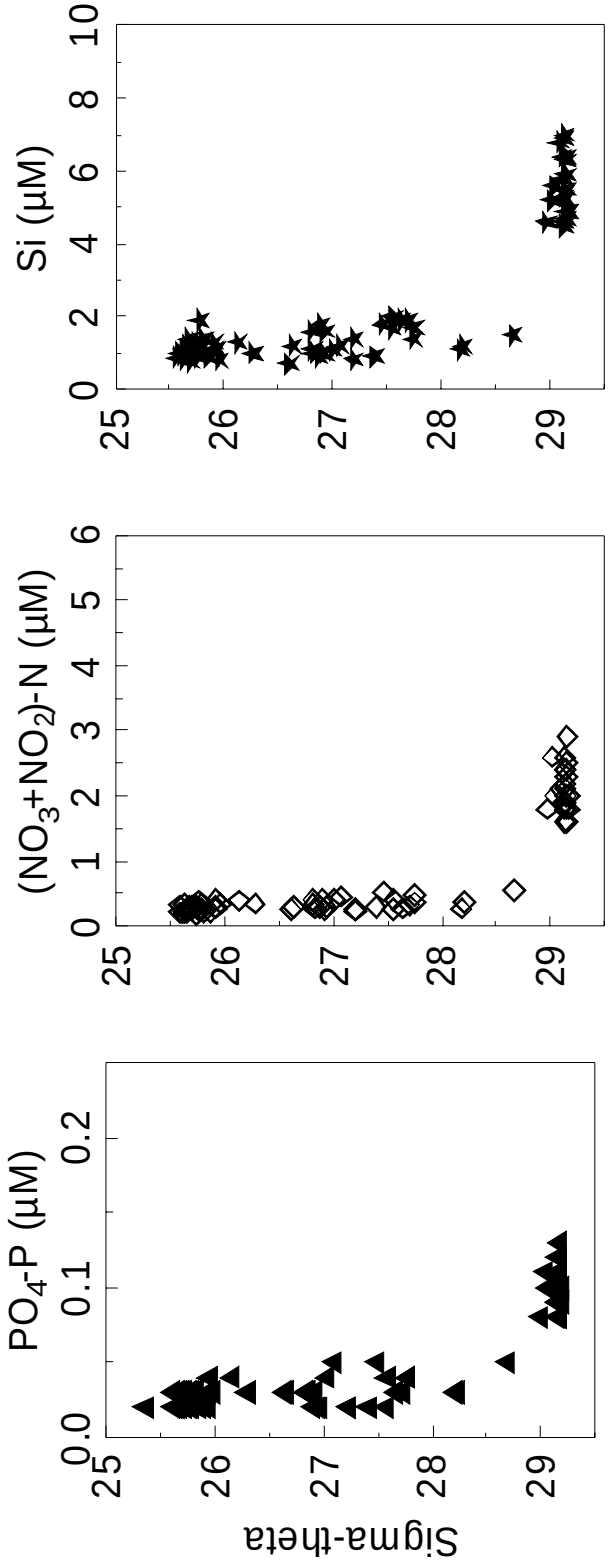

Figure 4.24 The plots of dissolved nutrients versus sigma-theta for the whole basin in July 1998

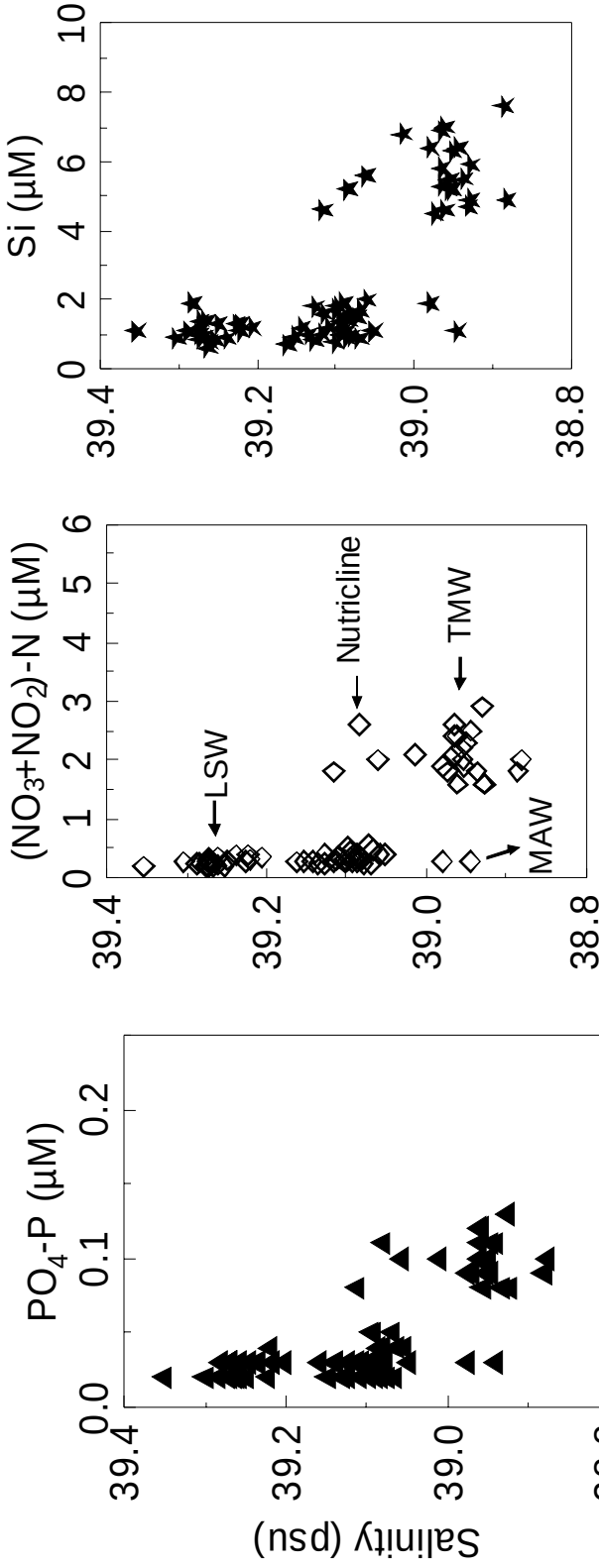

Figure 4.25 The plots of dissolved nutrients versus salinity for the whole basin in July 1998

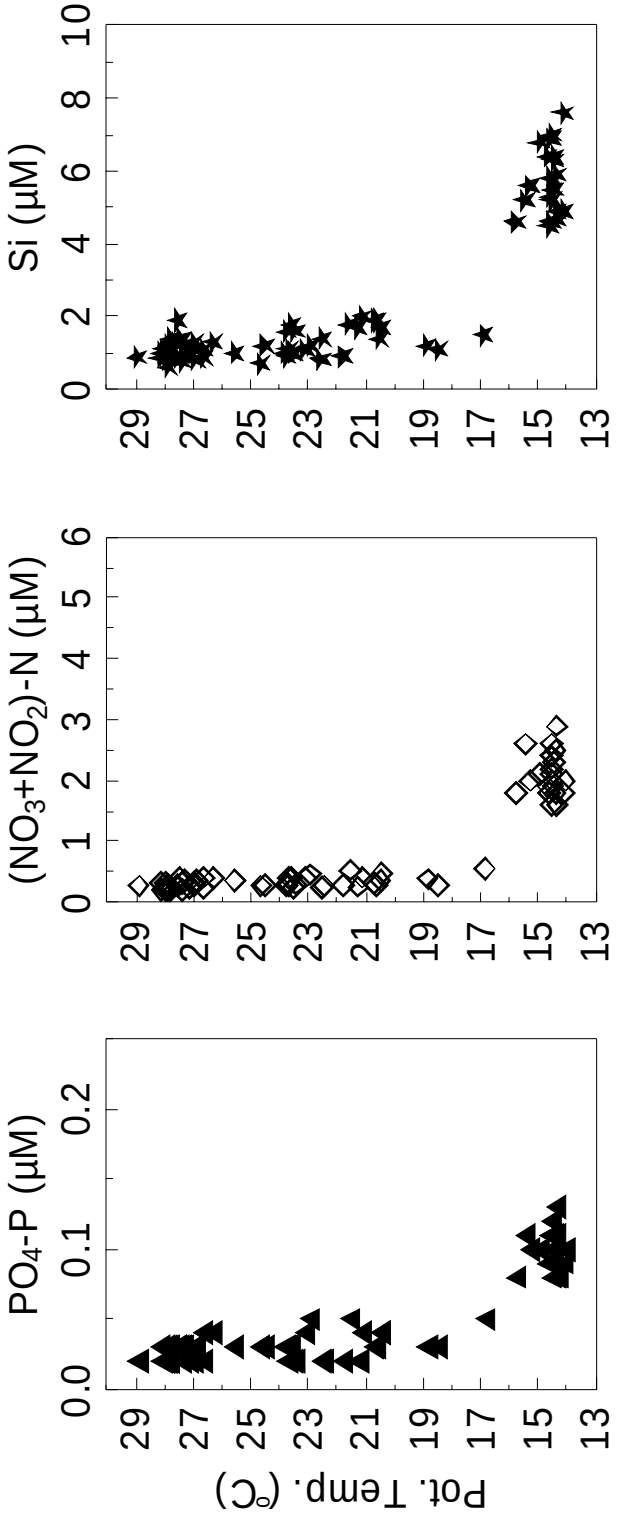

Figure 4.26 The plots of dissolved nutrients versus potential temperature for the whole basin in July 1998

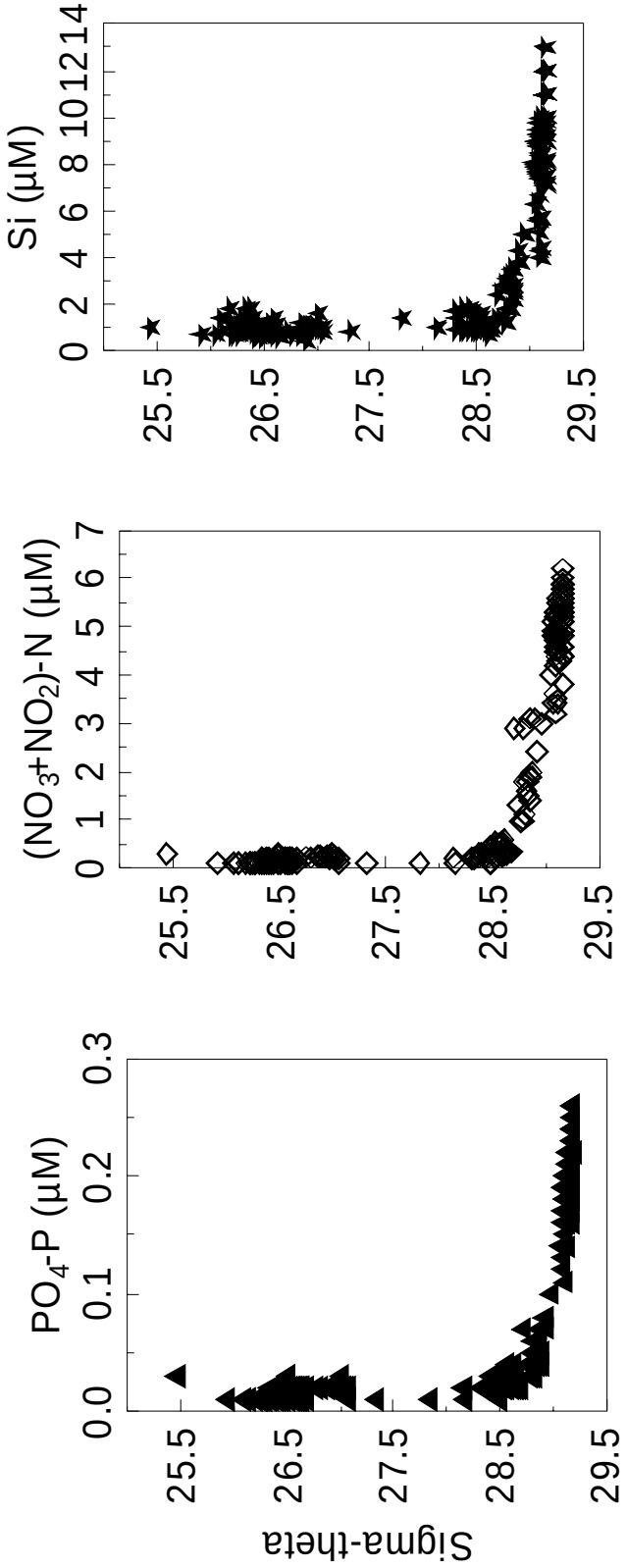

Figure 4.27 The plots of dissolved nutrients versus sigma-theta for the whole basin in October 2003

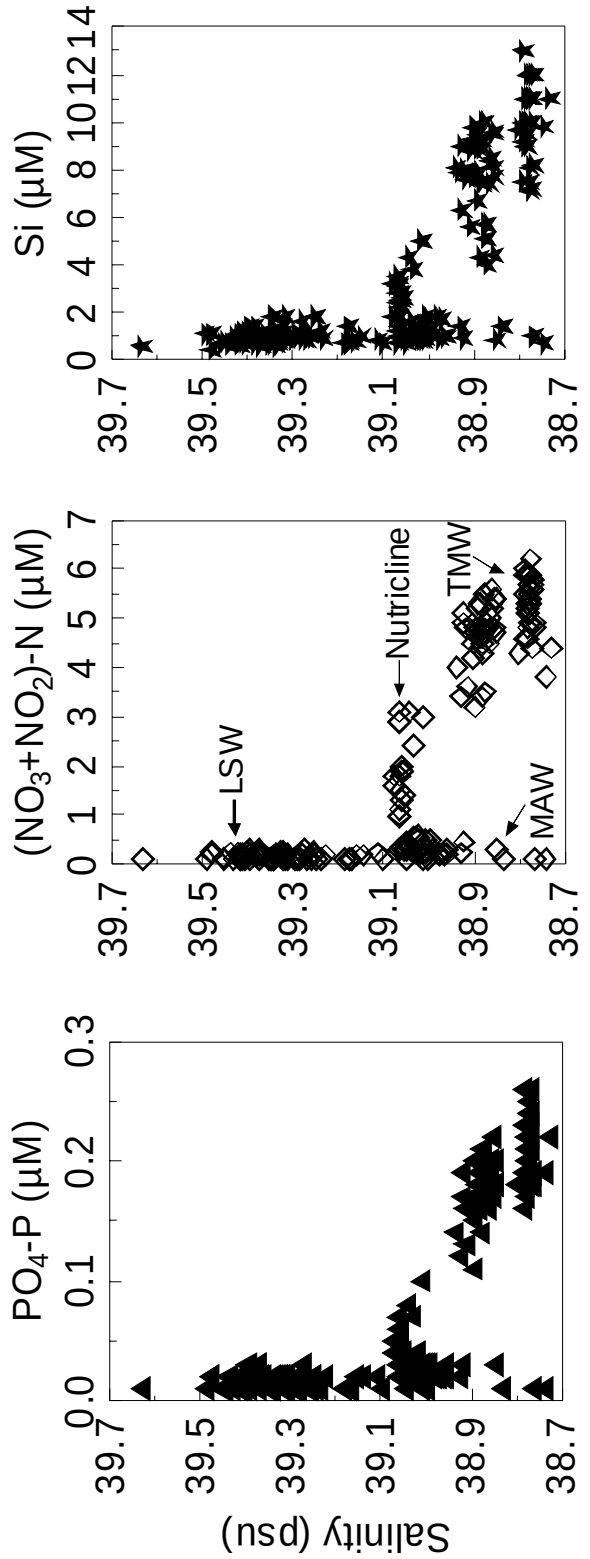

Figure 4.28. The plots of dissolved nutrients versus salinity for the whole basin in October 2003

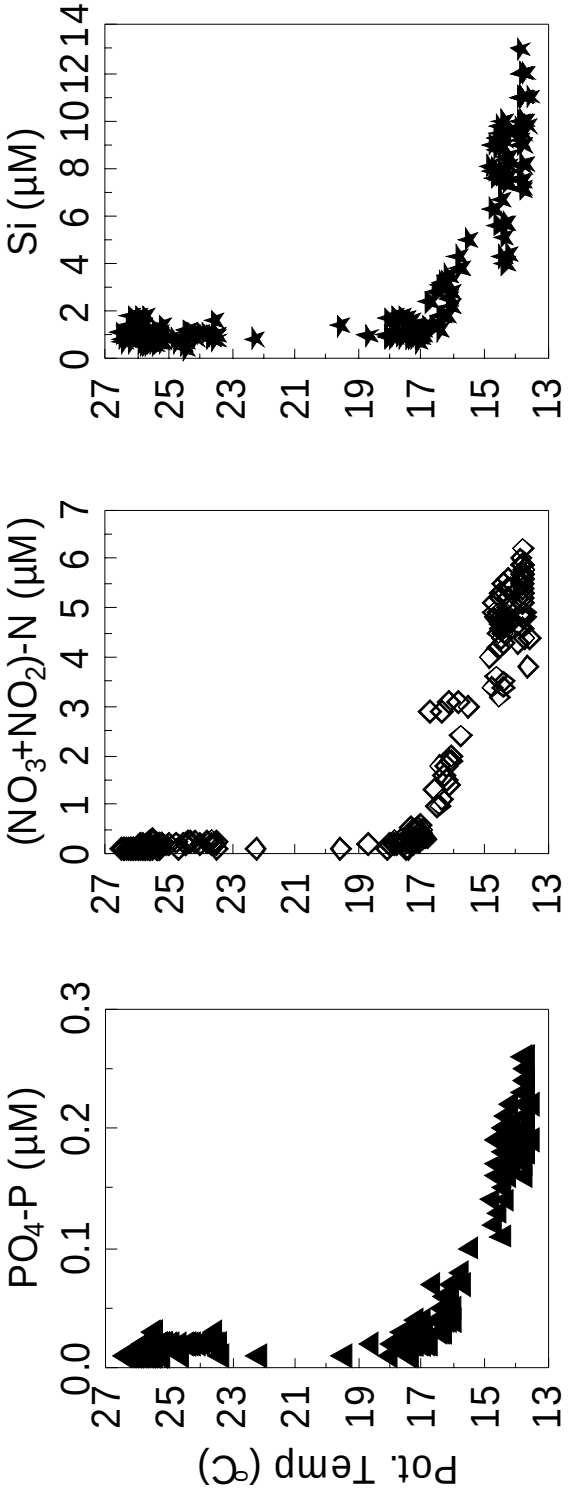

Figure 4.29 The plots of dissolved nutrients versus potential temperature for the whole basin in October 2003

The main nutricline, coinciding with the permanent pycnocline, is established just below the LIW layer at 200-250 m depths. In the TMW (S= 38.7-38.8 psu and T= 14°C), below the nutricline, there was a slight nitrate, phosphate maximum and then constant values of 5.5 μM nitrate and 0.22 μM phosphate. Silicate continued to increase slowly below the nutricline. The average silicate concentration was determined as 10 μM.

Comparison of nutrient profiles in Figure 4.30 (with the enlarged sigma-theta scales) reveals that the phosphate gradient zone appears at isopycnal surfaces ~0.05 density units greater than the nitracline and silicacline. The scatter, however, was more pronounced in the salinity dependent nutrient profiles because water masses with similar densities had regionally and seasonally varying salinities and temperatures. Thus, the nutricline formed with spatially and temporally variable thickness has different chemical concentrations at a given density and/or salinity surface from one location to another and from one year to another depending on the climatological conditions.

Similar results were reported by Yilmaz and Tugrul (1998) for the Levantine Basin; they related this apparent shift between the phosphacline and nitracline onsets either selective accumulation of labile nitrogen or from selective removal of phosphate at the permanent pycnocline. Heterotrophic and chemosynthetic activities in the lower pycnocline may contribute to the selective accumulation of labile dissolved organic nitrogen, which eventually oxidized to nitrate and may have caused high nitrate concentrations relative to phosphate.

The surface waters of the Cilician Basin are poor in nutrients for most of the year comparing the other areas of Levantine Basin The depth-averaged values for the surface layer were 0.3 μM for nitrate+nitrite and 0.03 μM for phosphate in May 1997 and July 1998 (Table 4.5). In October 2003, the upper layer was also poor in nutrients (NO_3+NO_2=0.16μM, PO_4=0.02μM).

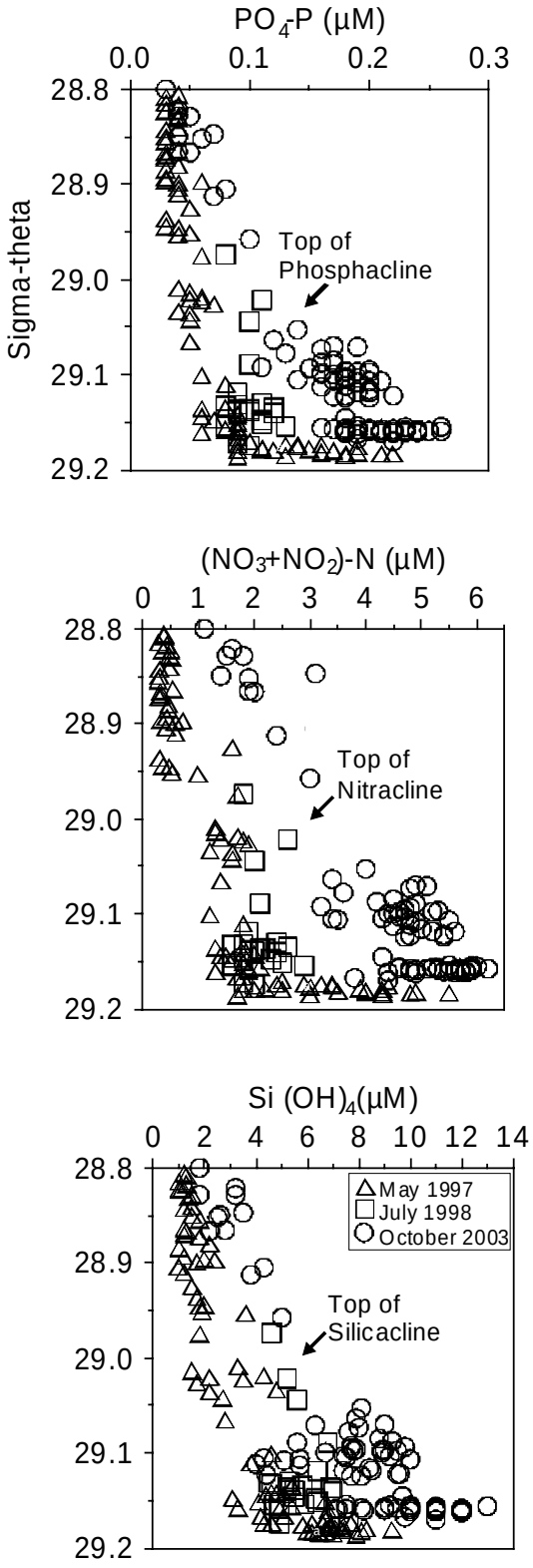

Figure 4.30. The plots of dissolved nutrients versus enlarged sigma–theta for the whole basin in May 1997, July 1998 and October 2003

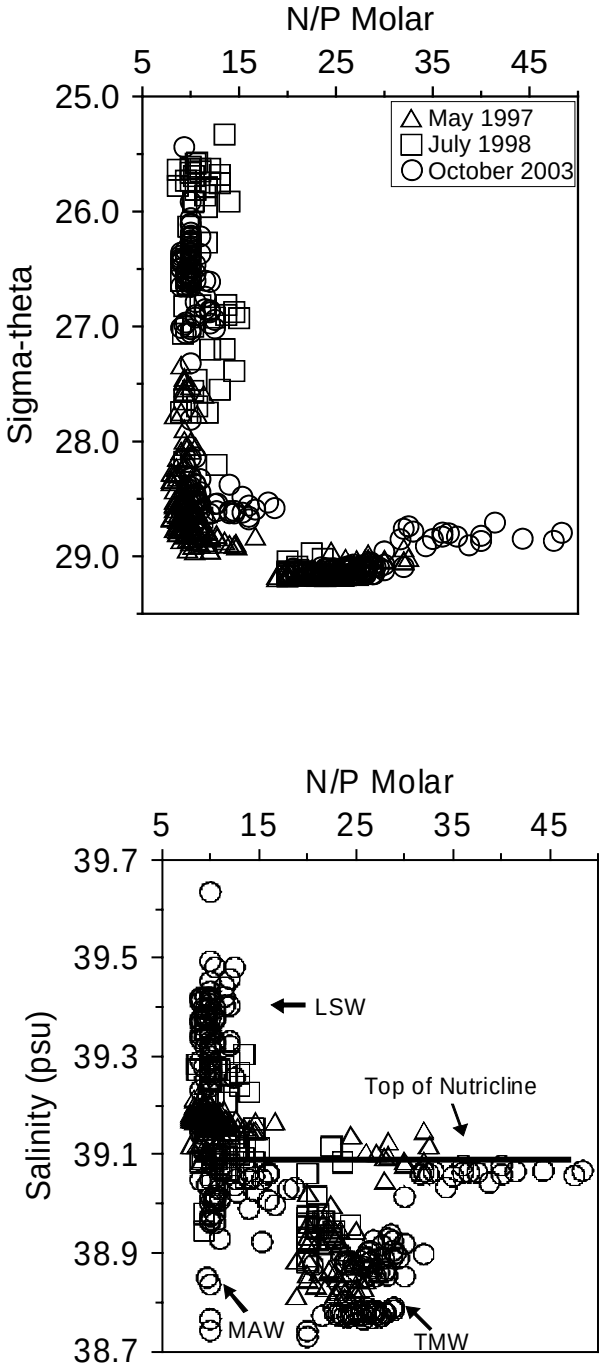

Figure 4.31 Salinity and sigma-theta versus N/P ratio in the sampling periods.

The silicate values always nearly 1 μM in the surface layer throughout the year. Concentrations in the TMW were recorded as 3.3 μM for nitrate, 0.14 μM for phosphate and 6.8 μM for reactive silicate in May 1997. During the July 1998 cruise, dissolved nutrient concentrations in the TMW (at a depth of 300m) were: 2.1, 0.10 and 5.7μM for nitrate, phosphate and silicate, respectively. In October 2003, the nutrient concentrations of TMW increased (NO_3+NO_2 = 5.3μM, PO_4 = 0.21μM, $Si(OH)_4$=10μM). The mean molar ratios of nitrate to phosphate (N/P) were calculated ~10-11 in the surface layer and ~21-25 in the TMW (Table 4.5).

Table 4.5 The average concentrations of dissolved nutrient elements (μM) and N/P molar ratios (NO_3+NO_2/PO_4) for the top of 500 m in the Cilician Basin

Period	Water Layer	PO_4-P	(NO_3+NO_2)-N	$Si(OH)_4$	N/P
May 1997	LSW	0.03±0.0004	0.28±0.005	1.0±0.03	9.5±0.09
	TMW	0.14±0.008	3.3±0.21	6.8±0.21	23±0.44
July 1998	LSW	0.03±0.001	0.31±0.01	1.2±0.05	11±0.24
	TMW	0.10±0.003	2.1±0.08	5.7±0.19	21±0.29
October 2003	LSW	0.02±0.0007	0.16±0.007	0.95±0.03	10±0.1
	TMW	0.21±0.004	5.3±0.10	10±0.25	25±0.38

The physical and chemical identities of the water masses, which are components of the Cilician Basin's circulation, are well presented by the θ-S analysis and the salinity dependent nutrient profiles. Apart from the temporal differences in the upper layer, the vertical structure remains almost unchanged and is formed by four basic water masses; the LSW, MAW, LIW and TMW. This is in agreement with the hydrographic data collected during 1995-1996 cruises in the south of Cyprus (Zodiatis, Theodorou, and Demetropoulos, 1998).

Below 100 m both the T/S and the nitrate, phosphate and silicate distributions in all of these three surveys did not possess appreciable seasonal variability. According to Codispoti (1989), a 'healthy' marine ecosystem should maintain an N/P ratio near 16/1. In our data, the mean N/P ratio ranges between 14.3 and 18.5 during May 1997,

July 1998 and October 2003, and is very consistent with those reported for the Southeastern Mediterranean (Krom et al. 1992; 1993; Yilmaz & Tugrul 1998). The phosphate and nitrate concentrations appeared to be markedly less than the concentrations (PO_4= 0.38 μM; NO_3+NO_2 =7.6 μM) reported for the western Mediterranean (Bethoux et al., 1992).

The molar ratios of nitrate to phosphate (N/P) in the water column of the Cilician Basin vary substantially with depth (Figure 4.31). In the surface layer, the ratio generally ranged between 8 and 20. In the MAW average of the N/P ratio is ~10. The N/P maximum (24.4-48.3) occurs near the top of nitracline, appeared at nearly 39.1 psu salinity and 29.0 kg/m^3 density surfaces. The maximum ratios originated from the apparent shift between the onsets of the nitracline and phosphacline depths. Similar maximum ratios were reported by Krom et al. (1992) for the southern Levantine basin; they attributed these maxima to the preferential uptake of reactive phosphate by planktonic species. Below the nutricline the N/P ratios decrease regularly and reach an almost constant deep value (~24-28) over the basin in the TMW.

The differences observed in the hydrological and chemical structure of the water column during May 1997, July 1998 and October 2003 indicate that the Cilician Basin is a dynamic system displaying pronounced seasonal and interannual fluctuations.

CHAPTER FIVE
CONCLUSIONS

5.1 CONCLUSIONS

In this study, physical parameters were used in conjunction with nutrient data to describe the water masses and circulation in the north of Cyprus and adjacent regions during late spring 1997, summer 1998 and fall 2003, and thus contribute to a better understanding of regional oceanography.

The synthesis of the three datasets has confirmed earlier conclusions but also revealed new features. Levantine Surface water, which is indicated a seasonal trend, has high salinity and high temperature as a result of the high rates of heating and evaporation. The Modified Atlantic Water appeared to be poorly defined during spring however it became better defined in summer and fall. There appeared to be no season related variations in the Levantine Intermediate Water and Transitional Mediterranean Water. While the LIW occurred at the depth of 300 m in 1991, it extending up to ~200 m after 1995, with a temperature of about 16°C and constant salinity (S=39.2 psu) in this study.

The topographic control would not be a major process controlling the flow structure. The results show that flow structure reflects highly dynamic temporal variability in the system. The differences in three circulation patterns may be associated with the mesoscale variability. The Cilician Basin circulation consists of sub-basin-scale gyres driven by thermohaline forcing and topography, and a number of energetic mesoscale eddies. Basin geometry and bottom topography could play important roles in the Cilician Basin circulation. The existence of an inter-annual variability in the circulation of the Cilician Basin is still arguable.

An AW trace at the eastern part of the Cilician Basin in July 1998 but it could not reach to the Lattakia Basin as a result of geostrophic circulation. Voluminous amount of AW penetrating is determined in the east of Cyprus in October 2003 and the

strong southward current carried the AW to the Lattakia Basin. In the May 1997, the AW signature in the Cilician Basin is lost because of wintertime mixing.

The nutriclines appear at specific density surfaces throughout the Cilician Basin even though their depths are well known to vary markedly in space and time. Interestingly, the upper boundary of the phosphate gradient zone is situated at greater density surfaces —by nearly 0.05 units— than the nitracline. Transitional Mediterranean Waters have relatively high N/P ratios; ~24-28 instead of 15 in the open ocean and 10 in the MAW. As nutrient deep concentration is greater than Levantine surface concentration, vertical movements in the Cilician Basin induce nitrogen enrichment of deep layer.

The current flows towards to the north and south along the eastern coast of Cyprus, on the western side of the Lattakia Basin in sampling periods. Transport of pollution does not affect coast of Northern Cyprus due to current direction. Coastal currents should be undertaken to ascertain in future studies for transportation of pollution in the coastal waters of Northern Cyprus.

REFERENCES

Aksu, A.E., Ulug, A., Piper, D.J.W., Konuk, Y.T., & Turgut, S., (1992). Quaternary sedimentary history of Adana, Cilician and Iskenderun Basins: northeast Mediterranean Sea. *Mar.Geol. 104,* 55-71.

Apel, J.R. (1987). *Principles of ocean physics (International Geophysics Series Vol.38).* Academic Press Limited, London

Becacos-Contos, T., (1977). Primary production and environmental factors in an oligotrophic biome in the Aegean Sea. *Marine Biology, 42,* 93-98.

Bergametti, G., E. Remoudaki, R. Losno, E. Steiner, B. Chatenet, & P. Buat-Menard, (1992). Source, transport and deposition of atmospheric phosphorus over the northwestern Mediterranean. *Journal of Atmospheric Chemistry, 14,* 501-513.

Bethoux, J.P., & Copin-Montegut, G., (1988). Phosphorus and nitrogen in the Mediterranean Sea: specificities and forecasting. *Oceanologica Acta, 9,* 75-78.

Bethoux, J.P., Morin, P., Madec, C., & Gentili, B., (1992). Phosphorus and nitrogen behavior in the Mediterranean Sea. *Deep Sea Res., 39* (9), 1641-1654.

Biju-Duval, B., Letouzey, J., & Montadert, L., (1979). Variety of margins and deep basins in the Mediterranean. In J.S. Watkins, L. Montadert, P.W. Dickerson (Ed.). *Geological and Geophysical Investigation of Continental Margins* (293-317). Am. Assoc. Pet. Geol. Mem. 29.

Brenner, S., Rozentraub, Z., Bishop, J., & Krom, M., (1991). The mixed layer/thermocline cycle of persistent warm core eddy in the Eastern Mediterranean. *Dynamics of Atmosphere and Oceans, 15,* 455-476

Carter, T. C., Flanagan, J. P., Jones, C. R., Marchant F. L., Murchison, R. R., Rebman J. H., Sylvester J. C., & Whitney J. C., (1972). A new bathymetric chart and physiography of the Mediterranean Sea. In J.D Stanley, (Ed.) *The Mediterranean Sea: A Natural Sedimentation Laboratory* (1-23). Stroudsburg, Pennsylvania; Dowden, Huchingson&Ross, Inc.

Codispoti, L.A., (1989). Phosphorus vs. nitrogen limitation of new and export production. In W.H Berger, V.S. Smetacek, and G. Wefer, (Eds.), *Productivity of the ocean: present and past* (377-394) Wiley.

Coste, B., Le Corre, P., & Minas, H.J., (1988). Re-evaluation of the nutrient exchanges in the Straight of Gibraltar. *Deep Sea Res., 35,* 767-775.

Defant A., (1941). Die absolute topographie des physikalischen meeresniveanus und der druckflächen sowie die wasserbewegungen in raum des Atlantischen Ozeans. *Deutsche Atlantische Expedition 'Meteor' 1925-1927,* 191-260.

Earth probes TOMS. Absorbing Aerosol Index. (n.d.) Retrieved 9 December 2003 from ftp://jwocky.gsfc.nasa.gov/pub/tmp/meduse/.

Ediger, V., Evans, G., & Ergin, M., (1997). Recent surficial sediments of the Cilician Basin (Turkey), northeastern Mediterranean. *Cont. Shelf Res., 17,* 1659-1677. Retrieved November 19, 2004, from Elsevier ScienceDirect database.

Emery, K. O., Heezen B. C., & Allan T.D., (1966). Bathymetry of the eastern Mediterranean Sea. *Deep-Sea Research, 13,* 173-192.

Evans, G., Morgan, P., Evans, W.E., Evans, T.R., & Woodside, J.M., (1978). Faulting and halokinetics in the northeastern Mediterranean, between Cyprus and Turkey. *Geology, 6,* 392-396.

Evans, G., Lane-Serff, G.F., Collins, M.B., Ediger, V., & Pattiaratchi, C.B., (1995). Frontal instabilities and suspended sediment dispersal over the shelf of the Cilician Basin, southern Turkey. *Mar.Geol,. 128*, 127-136.

Feliks Y. & Itzikowitz S., (1987). Movement and geographical distribution of anticyclonic eddies in the eastern Levantine basin. Deep Sea Research Part A. Oceanographic Research Papers. 34 (9), 1499-1508

Grasshoff, K., Ehrhardt, M., & Kremling, K., (1983). Methods of Seawater Analysis. Second Revised and Extended Edition. Verlag Chemie, Weinheim.

Hetch, A., Pinardi, N. and Robinson, A.R., (1988). Currents, water masses, eddies, and jets in the Mediterranean Levantine Basin. *J. Phys. Oceanogr., 18,* 1320-1352.

Hsu, K.J., & Bernoulli, D., (1978). Genesis of the Tethys and the Mediterranean. *Init.Rep. DSDP 42*, 943-949.

Ignatiades, L. 1969. Annual cycle, species diversity and succession of phytoplankton in lower Saronicos Bay, Aegean Sea. *Marine Biology, 3:* 196-200.

IMST, 1998; “Ecological investigation of coastal water in the Northern Cyprus of Turkish Republic” Project. The Ministry of Agriculture and Forestry (in Turkish).

IMST, 1998. “Ecological investigation of coastal water in the Northern Cyprus of Turkish Republic” Project. The Ministry of Agriculture and Forestry (in Turkish).

IMST, 2003. “Ecological investigation of coastal water in the Northern Cyprus of Turkish Republic” Project. The Ministry of Agriculture and Forestry (in Turkish).

Krom, M.D., Kress N., & Brenner, S., (1991). Phosphorus limitation of primary productivity in the eastern Mediterranean. *Limnol. Oceanogr., 36,* 424-432.

Krom, M.D., Brenner, S., Kress, N., Neori, A., & Gordon, L.I., (1992). Nutrient dynamics and new production in a warm core eddy from the Eastern Mediterranean Sea. *Deep Sea Research, 39* (3/4), 467-480.

Krom, M.D., Brenner, S., Kress, N., Neori, A., & Gordon, L.I., (1993). Nutrient distributions during an annual cycle cross a warm core eddy from the E. Mediterranean Sea. *Deep Sea Research, 40* (4), 805-825.

Krom, M.D., Herut, B., Mantoura, R.F.C., 2004. Nutrient budget for the Eastern Mediterranean: implications for P limitation. *Limnology and Oceanography 49*, 1582– 1592.

Kubilay, N., (1996). The Composition of atmospheric aerosol over the eastern Mediterranean: The coupling of geochemical and meteorological parameters. PhD Thesis, 219 pp, IMS-METU, Turkey.

Kubilay, N., Nickovic, S., Moulin C., & Dulac, F., (2000). An illustration of the transport and deposition of mineral dust onto the eastern Mediterranean. *Atmospheric Environment 34*, 1293-1303.

Lascaratos, A., Roether, W., Nittis K., & Klein B., (1999). Recent changes in deep water formation and spreading in the eastern Mediterranean Sea: a review. *Prog. Ocean., 44,* 5–36. Retrieved October 22, 2004, from Elsevier ScienceDirect database.

Loye-Pilot, M.D., Martin, J.M., & Morelli, J., (1990). Atmospheric input of inorganic nitrogen to the western Mediterranean. *Biogeochemistry, 9,* 117-134.

MacIsaac, J. J., & Dugdale, R. C., (1972). Interaction of light and inorganic nitrogen in controlling nitrogen uptake in the sea. *Deep-Sea Research, 19,* 202-232.

Malanotte-Rizzoli, P., Manca B.B., Ribera d'Alcala, M., Theocharis, A., Brenner, S., Budillon, G., et al., (1999). The Eastern Mediterranean in the 80s and in the 90s: the big transition in the intermediate and deep circulation. *Dynamics of Atmosphere and Oceans, 29* (2–4): 365–395. Retrieved October 22, 2004, from Elsevier Science Direct database.

Mamayev, O.I., (1975). Temperature Salinity Analysis of World Ocean Waters, Elsevier Oceanography Series, 11, Amsterdam-Oxfrord-New York: Elsevier Scientific Publishing Company.

McGill, D.A., (1969). A Primarily study of the Oxygen and Phosphate distribution in the Mediterranean Sea. *Deep Sea Res., 8* (3/4), 259-269.

Migon, C., & Sandroni, V., (1999). Phosphorus in rainwater: Partitioning inputs and impact on the surface coastal ocean. *Limnol. Oceanogr., 44*(4), 1160-1165.

Neumann,G., (1968). *Ocean Currents*. Elsevier Scientific Publ. Co. NY 352p.

OMC: Create a Map (n.d.). Retrieved 10 October 2006 from http://www.aquarius.geomar.de/omc/make_map.html.

Ovchinnikov, I.M., (1984). The Formation of Intermediate Water in the Mediterranean. *Oceanology, 24,* 168–173.

Ozsoy, E., Hecht, A., & Unluata, U., (1989). Circulation and hydrography of the Levantine Basin: Results of POEM coordinated experiments 1985-1986. *Prog. Oceanogr., 22*, 125–170.

Ozsoy E., Hecht, A., Unluata, U., Brenner, S., Oguz, T., Bishop, et al., (1991). A review of the Levantine Basin circulation and its variability during 1985-1988. *Dynamics of Atmosphere and Oceans, 15,* 421-456.

Ozsoy, E., Hecht, A., Unluata, U., Brenner, S., Sur, H. I., Bishop, J., et al., (1993). A synthesis of the Levantine Basin circulation and hydrography, 1985-1990. *Deep Sea Research, 40* (6): 1075-1119.

POEM Group, (1992). General circulation of the Eastern Mediterranean. *Earth Sci. Rev., 32*, 285-309.

Practical Salinity Scale Equations, (1980). IEEE, *Journal of Oceanic Engineering, 5* (1): 13-14.

Quetel, C.R., Remoudaki, E., Davies, J.E., Miquel, J.C., Fowler, S.W., Lambert, C.E., et al. (1993). Impact of atmospheric deposition on particulate iron flux and distribution in northwestern Mediterranean waters. *Deep Sea Res., 40*, 989-1002.

Redfield, A.C., Ketchum, B.H, & Richards, F.A., (1963). The influence of organisms on the composition of seawater. In M.N. Hill (Ed.), *The sea, ideas and observations on progress in the study of the seas* (26-77). New York: Wiley

Robinson, A.R., Hecht, A., Pinardi, N., Bishop, J., Leslie, W.G., Rosentroub, Z., et al., (1987). Small synoptic/mesoscale eddies and the energetic variability of the Eastern Levantine Basin. *Nature, 327*, 131-134.

Robinson, A.R., Golnaraghi, M., Leslie, W.G., Artegiani, A., Hecht, A., Lazzoni, E., et al., 1991. The Eastern Mediterranean general circulation: features, structure and variability. *Dynamics of Atmospheres and Oceans, 15*, 215-240.

Roether, W., Manca, B.B., Klein, B., Bregant, D., Georgopoulos, D., Beitzel, V., et al., (1996). Recent changes in the Eastern Mediterranean deep waters. *Science, 271*, 333–335.

Roussenov, V., Stanev, E., Artale, V., & Pinardi, N., (1995). A seasonal model of the Mediterranean Sea general circulation. *J. Geophys. Res., 100,* 13515–13538.

Salihoglu, I., Saydam C., Basturk, O., Yılmaz, K., Gocmen, D., Hatipoglu, E., et al., (1990). Transport and distribution of nutrients and chlorophyll-a by mesoscale eddies in the northeastern Mediterranean. *Mar. Chem., 29,* 375-390.

Shaw, H.F., (1978). The clay mineralogy of the recent surface sediments from the Cilician Basin, north-eastern Mediterranean. *Mar.Geol., 26,* M51-M58.

Shaw, H.F., & Bush, P.R., (1978). The mineralogy and geochemistry of the recent surface sediments from the Cilician Basin, north-eastern Mediterranean. *Mar.Geol., 27*, 115-136.

Shtokman, V.B., (1944). Geometrical Properties of θ-S curves in the mixing of three water masses in an infinite sea. *Izv. Akad. Nauk S.S.S.R., 13* (8) (in Rusian).

Stricland, J.D.H., & Parsons, T.R., (1972). *A practical Handbook of seawater Analysis*. 2nd edition Bulletin 167. Fisheries Research Board of Canada: Ottowa.

Takahashi, T., Broecker, W.S., & Langer, S., (1985). Redfield ratio based on chemical data from isopycnal surfaces. *J. Geophys. Res., 90*(C4), 6907–6924.

Talbot, R. W., Harris, R.C., Brawl, E.V., Gregory, G.L., Debaucher, D.I., & Beck, S.M., (1986). Distribution and geochemistry of aerosols in the tropical North Atlantic troposphere: Relationship to Saharan dust. *J. Geophys. Res., 91*, 5173-5182.

The Oceanography Course Team, (1997). *Seawater: Its Composition, Properties and Behaviour* (Second Edition). The Open University, England: Butterworth-Heinemann

The Oceanography Course Team, (1993). *Ocean Circulation*. The Open University, England: Pergamon Press.

Theocharis, A., Georgopoulos, D., Lascaratos, A., & Nittis, K., (1993). Water masses and circulation in the central region of the Eastern Mediterranean: eastern Ionian,

south Aegean and northwest Levantine, 1986–87. *Deep-Sea Research, Part II 40* (6), 1121– 1142. Retrieved September, 10, 2004 from Elsevier ScienceDirect database.

Theocharis, A., Balopoulos, E., Kioroglou, S., Kontoyiannis, H., & Iona, A., (1999). A synthesis of the circulation and hydrography of the south Aegean Sea and the Straits of the Cretan Arc (March 1994–January 1995). *Progress in Oceanography 44*, 469–509.

Theocharis, A., Klein, B., Nittis K., & Roether, W., (2002). Evolution and status of the Eastern Mediterranean Transient (1997–1999). *Journal of Marine Systems, 33-34*, 91-116. Retrieved October, 17, 2004 from Elsevier ScienceDirect database.

Tselepides, A., Zervakis, V., Polychronaki, T., Danovaro, R., & Chronis, G., (2000). Distribution of nutrients and particulate organic matter in relation to the prevailing hydrographic of the features of the Cretan Sea (NE Mediterranean). *Progress in Oceanography 46*, 113– 142. Retrieved October, 17, 2004 from Elsevier ScienceDirect database.

Thingstad T. F., & Rassoulzadegan, F., (1995). Nutrient limitations, microbial food webs and 'biological C-pumps': suggested interactions in a P-limited Mediterranean. *Marine Ecology Progress Series, 117*, 299-306.

Unluata, U. (1986). A review of the physical oceanography of the Levantine and the Aegean basins of the Eastern Mediterranean, in relation to monitoring and control of pollution. Institute of Marine Sciences, METU Technical Report, 55.

Wong, H. K., Zarudzki, E. F.K., Philips, J. D., & Giermann, G. K.F., (1971). Some geophysical profiles in the eastern Mediterranean. Geological Society of *American Bulletein, 82*, 91-100.

Yilmaz, A., & Tugrul, S., (1998). The effect of warm core eddies on the distribution and stoichiometry of dissolved nutrient in the northeastern Mediterranean. *Journal*

of Marine Systems, 16, 253-268. Retrieved November 3, 2003, from Elsevier ScienceDirect database.

Zodiatis G., Theodorou, A., & Demetropoulos, A., (1998). Hydrography and Circulation south of Cyprus in late summer 1995 and in spring 1996. *Oceanologica Acta, 21*(3), 447-458.